2011

A Microfluidics Approach to Novel Polymeric Microspheres Reinforced with n-Ti02

Sepideh Rezvani

A Microfluidics Approach to Novel Polymeric Microspheres Reinforced with n-TiO_2

(Spin Title: Microfluidics-Novel polymeric microspheres-n-TiO_2)

(Thesis format: Monograph)

by

Sepideh Rezvani

Graduate Program

in

Engineering Science

Department of Chemical and Biochemical Engineering

A thesis submitted in partial fulfillment

of the requirements for the degree of

Master of Engineering Science

School of Graduate and Postdoctoral Studies

The University of Western Ontario

London, Ontario, Canada

2011

THE UNIVERSITY OF WESTERN ONTARIO

SCHOOL OF GRADUATE STUDIES AND POSTDOCTORAL STUDIES

CERTIFICATE OF EXAMINATION

Supervisor	Examiners
Dr. Paul A. Charpentier	Dr. Madhumita (Mita) Ray
Supervisory Committee	Dr. Lars Rehmann
Dr. Madhumita (Mita) Ray	Dr. Jun Yang

The thesis by

SEPIDEH REZVANI

Entitled:

A Microfluidics approach to novel polymeric microspheres reinforced with n-TiO_2

is accepted in partial fulfilment of the

requirements for the degree of

Master of Engineering Science

Date_____ _____ Chair of

the Thesis Examination Board

ABSTRACT

Polymethylmethacrylate (PMMA) is a brittle polymer used for both commercial dental and bone cement applications. Its poor mechanical properties leads to implant failures requiring revisions which is a tremendous current problem as we live longer and more active lives. The objective of this work was to produce microspheres of PMMA containing titanium dioxide (TiO_2) nanofillers that have the potential for enhancing the mechanical properties of these cements. To make the TiO_2 nanofillers organophillic to be compatable with PMMA, a variety of bifunctional molecules were examined for coordination to the TiO_2 nanospheres through a –COOH functionality. These bifunctional molecules have an additional vinyl group that can be used for subsequent 'grafting from' polymerization from the TiO_2 surface after co-ordination. TGA (thermogravimetric analysis) and water/MMA bilayer experiments were examined to investigate the coordination reaction and stability of the resulting nanostructures in MMA monomer. Then, to provide uniform polymer microspheres containing well dispersed nano TiO_2 for integration into the bone cements, a microfluidics approach was examined using interfacial polymerization. A T-junction microfluidics reactor was designed which can control the size of microspheres by adjusting the reactor pressure, flow rate of inlets, as well as the geometry of the micro-channels. A preliminary computational fluid dynamics (CFD) model was developed for the theoretical and experimental description of the polymerization process. This approach offers a potentially lower cost, adjustable process for making microsphere nanocomposites compared to other more traditional polymerization approaches.

Key Words: Titania powders, Functionalization, Polymer microspheres, Microfluidics, interfacial polymerization, CFD modeling

Dedication

To the people in my life who have always believed in me,

seen me at my best and worst, and always stood by me.

Acknowledgements

There are many individuals that I would like to acknowledge for their help, support, encouragement, and patience throughout the past two years. Firstly, I would like to express my great appreciation and respect to my advisor, Dr. Paul Charpentier, who through numerous means provided me guidance, support, respect, and friendship through the progression of this research project. Without him, none of this would have been possible.

My parents, Maryam and Yazdi, have been a constant source of support during my postgraduate years, and this thesis would certainly not have existed without them. Special thanks to my mother Maryam for believing in me and being my support pillar always and my sister, Sahar, who has been my best friend.

I would also like to extend acknowledgement to my fellow group members at the University of Western Ontario, who provided their ongoing support, questions and suggestions.

Table of Contents

List of Figures

List of Tables

List of Abbreviations, Symbols

CFD : computational fluid dynamics

DSC: differential scanning calorimetry

DLS :digital light scattering

FTIR: Fourier transform infrared spectroscopy

GPC: gel permeation chromatography

IEP : isoelectric point

MMA: methyl methacrylate

MA: methacrylic acid

n-TiO_2 fibers: titania nanofibers

n-TiO_2 tubes : titania nanotubes

n-TiO_2 powders: titania nanopowders

PMMA: poly(methyl methacrylate)

PVA: poly(vinyl alcohol)

PDMS: polydimethylsiloxane

PS: polystyrene

SEM: scanning electron microscopy

TEM: transmission electron microscopy

TGA: thermogravimetric analysis

THF – tetrahydrofuran

XRD: X-ray diffraction

Nomenclature

a – area (m^2)

E – energy (J)

f – frequency (Hz)

h – height (m)

[M] – monomer concentration (mol/L)

$[M]_o$ – initial monomer concentration (mol/L)

T_i - initial temperature of decomposition (°C)

T_i^{max} - maximum temperature of decomposition(°C)

v – velocity (m/s)

γ – surface tension (N/m)

Ca- Capillary number

Re- Reynolds number

Pe- Peclet number

CHAPTER 1: INTRODUCTION

1.1. Overview

The focus of this thesis was to develop poly (methyl methacrylate) (PMMA) microspheres reinforced with commercially available titanium dioxide nanopowders (n-TiO_2) using a microfluidics method of polymerization. PMMA is a brittle polymer used in both commercial dental and bone cement applications. However, its poor mechanical properties leads to implant failures and required revisions which is a tremendous current problem as we live longer and more active lives. In this work, nanostructured titanium dioxide (TiO_2) is examined as a PMMA filler for enhancing its mechanical properties. A novel functionalization route was utilized to make the hydrophilic TiO_2 nanomaterials compatible with the hydrophobic organic PMMA matrix. Applying this route, methacrylic acid (MA) was used for its bifunctional characteristics having both a carboxyl group for coordination and electrostatic interaction with titania and a vinyl group for subsequent polymerization with methyl methacrylate (MMA) monomer. A variety of bifunctional molecules are examined for coordination to the TiO_2 through a –COOH functionality with a vinyl functional group used for subsequent polymerization; 2-carboxyethyl acrylate, 10-undecenoic acid, and methacrylic acid each have these groups with different chain lengths to also investigate the effect of chain length on steric stabilization. TGA and water/MMA bilayer experiments were examined to investigate the coordination reaction and stability of the nanostructures in MMA monomer.

In order to synthesize the polymeric microspheres, a T-junction microfluidics reactor was designed which can control the size of the microspheres by adjusting the flowrates of the reactants (oil/water phases) and the geometry of the microchannels. This approach offers a potentially lower cost, tuneable process compared to other more traditional polymerization

approaches. In this chapter the motivation and the potential application of the synthesis method are addressed.

Essential studies on the resulting functionalized nanomaterials were carried out using various physico-chemical and analysis testing methods including TGA, FTIR, RAMAN, DLS, SEM and TEM. Polymer particles produced by the microfluidic method were studied using TGA, FTIR, DLS, SEM, TEM, GPC along with light microscope (Ziess) and RAMAN spectroscopy. Computational fluid dynamics (CFD) modeling was used to represent the flow pattern of the fluids in the system with respect to changes in the geometry of the Micro-TEE reactor.

1.2. Literature review

1.2.1 PMMA Used for Bone Cements

There is a need for a new generation of bone cements with long life spans as the current implant life span is only 10-20 years which is not acceptable for today's active life style and quality of life for people that live significantly longer lives than previous generations. Figure 1.1 shows the evolution of bone cements in the past century.

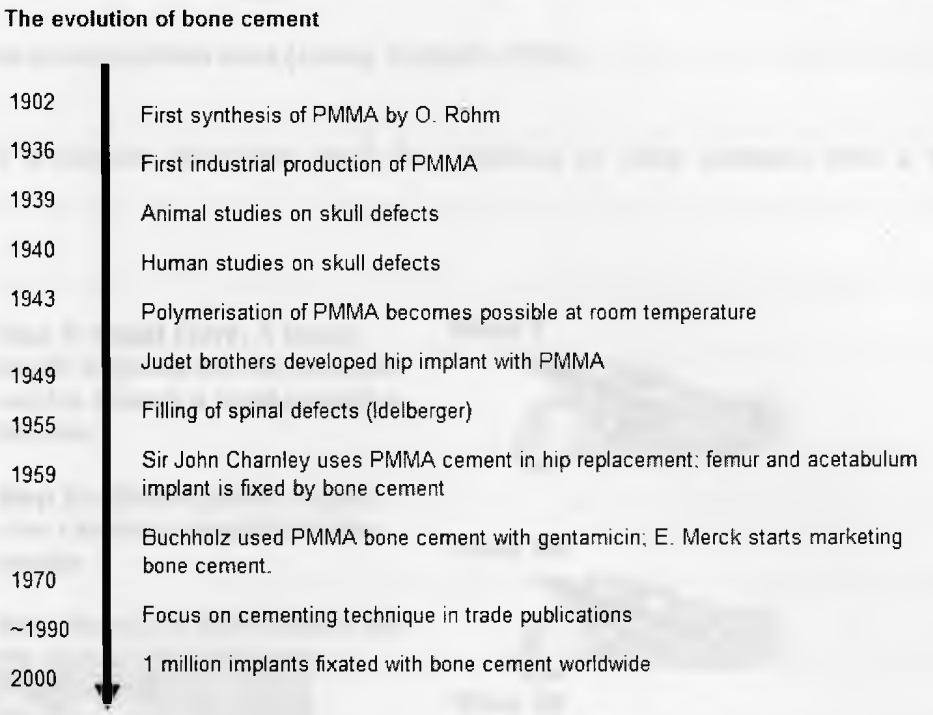

Figure 1.1: The evolution of bone cement (Parallax medical 2011).

The PMMA based bone cements currently used have low mechanical properties due to incompatibility between the higher polarity ionic radioopaqe fillers with the low polarity polymeric resin (Khaled 2009). The chemical bond between the acrylic matrix and the nanofillers is expected to reduce the production of abrasive nanofiller debris in the tissue area surrounding the prosthesis joint (Steinbacher, McQuade 2006). However, there is a lack of chemical bonding along with poor wetting and weak interfacial interactions between the inorganic particulates and the non-polar polymer matrix. This means that the filler particles act as stress concentration sites (Puska et al. 2003). Therefore when stress is applied to the bone cement, these sites facilitate implant failure. Thus there is a need for alternative radio-pacifiers that can also act as reinforcing agents for PMMA bone cements. These efforts have not been very successful to date because of the large size of the fillers, poor filler-bone cement matrix

bonding (and subsequent de-bonding), non-uniform filler material distribution, and the pores functioning as stress concentration sites (Jones, Rizkalla 1996).

Figure 1.2 shows a current procedure used for injection of bone cements into a vertebra (BIOMET 2011).

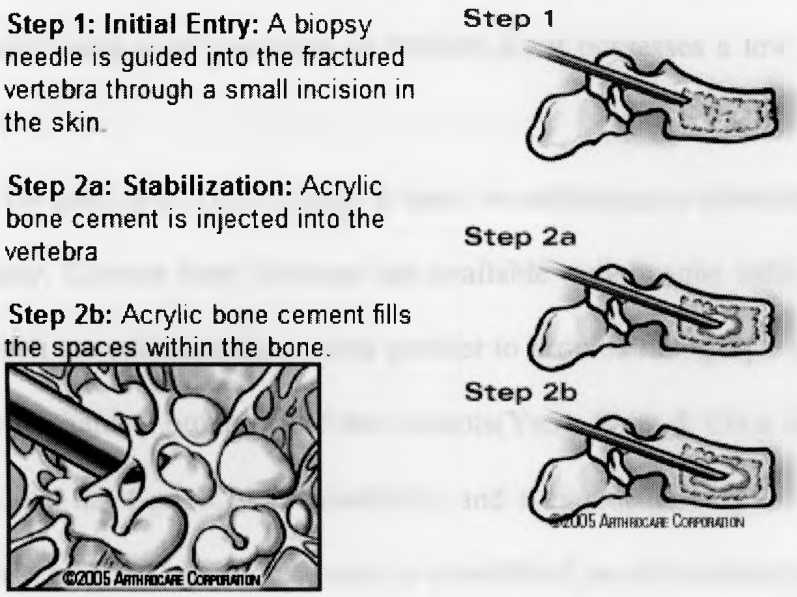

Figure 1.2: Bone cement injection procedure.

PMMA is a representative material used for commercial bone cements due to its self-hardening ability and excellent mechanical properties compared to other polymers. However, this application is restricted to the bone cement itself due to the bio-inertness of PMMA; no chemical or biological bonding occurs at the interface between the PMMA and bone causing the PMMA to wear down as a result of repeated interfacial movement. As a result, the use of PMMA becomes one of the factors contributing to osteolysis and subsequent loosening of the implant. Therefore, many studies have been conducted to provide osteoconductivity (i.e. comprehensive

bone growth) to the PMMA bone cement by introducing bioactive ceramic fillers (Khaled 2009). The mechanical features of ceramics and glass includes high strength and hardness but also low fracture toughness, i.e. brittleness because the atoms in ceramics are connected to one another through strong and directional covalent and coordination bonding. However, the composite comprised of PMMA and bioactive ceramic particles shows slightly higher brittleness compared to composites made using other polymers as PMMA itself possesses a low fracture toughness (Lee, Rhee 2009).

For a material to be used as a bone cement; it must be radiologicaly detectable for a later joint replacement surgery. Current bone cements use available radioopaque salts such as $BaSO_4$ or ZrO_2 particles which are added to the cement powder to provide radiopaque properties, but they also result in low mechanical properties of the cements(Yang, Shim & Choe 2005). Titanium and titanium-based alloys have good biocompatibility and their outstanding mechanical properties are similar to those of bone, therefore titania is considered as an excellent material for dental implants, artificial hip joints, and bone screws. Furthermore, an oxide layer formed upon exposure to air results in an excellent inertness of its surface, allowing it to willingly heal into the bone tissue. Regardless of all these excellent properties, a true adhesion between the bone and the metal surface has not yet been observed. Considering the topographical modifications of titanium oxide surfaces, the presence of the titanium oxide in the polymer matrix increases the surface roughness. The modification of the surface chemistry of titanium oxide includes different possible approaches that allows the tailoring of surface properties (Pasqui et al. 2007). The next section explains the need for reinforcing the PMMA polymer with nanofillers for enhanced properties.

1.2.2 Polymer-Nanopowder Composites Synthesis

Polymer systems are widely used in a variety of applications due to their unique and advantageous attributes such as: ease of production, low cost, light weight, ductile nature, and easy processability (Ginebra et al. 2002). However, polymers have a lower modulus and strength compared to metals and ceramics. One way to improve their mechanical properties is by reinforcement with fillers. Traditionally, composites were reinforced with micron sized fillers, but recently scientific interest has focussed on nanoscale fillers. This is due to the nanofillers high surface to volume ratios which can increase the number of particle-matrix interactions increasing the effects on the overall material properties. Generally, the material properties of a polymer nanocomposite are superior to those of the corresponding micro-composite. However, a significant challenge with the use of nanoparticles is their high propensity for agglomeration. One solution to prevent the agglomeration is steric stabilization (Achilleos, Vamvakaki 2010). The stabilization of colloidal particles can be achieved by attaching macromolecules to the surfaces of the particles. To keep the nanoparticles separated, particles can be coated by polymer chains which are secured at one end to the nanomaterials surface. If the density of these chains is high enough, the chains extend from the surface to avoid overlapping one another, where the osmotic pressure between the two stabilized particles acts as a spring, providing the necessary repulsive force to keep the nanoparticles separated.

TiO_2 nanoparticles are of interest as fillers for PMMA because TiO_2 is nontoxic and it promises to create chemical and biological hybrid nanocomposites for cements that can be further used to initiate intercellular processes (Paunesku 2003). There are three ways for dispersion of nanopowders in polymers. The first method is direct mixing or blending of the polymer and the nanopowder either as discrete phases (known as melt mixing) or in solution (solution mixing). Although these methods are successful, they have some drawbacks as these processes build up

relatively weak interaction forces between the polymer and the nanopowder with nanopowders having a strong tendency to aggregate. Hence, dispersion is normally only successfully achieved after the surface of the inorganic nanopowders is modified. As well, the solution methods can have limitations for some polymers as there is a rapid increase in solution viscosity with the addition of a few volume fractions of nanopowders. Some of the limitations of melt mixing can be overcome if both the polymer and the nanoparticles are dissolved or dispersed in solution. This allows modification of the particle surface without drying, which reduces particle agglomeration. After dispersion, the polymer nanoparticle solution can then be cast into a solid, or isolated from solution by solvent evaporation or precipitation. Further processing can also be done using conventional polymer processing techniques such as extrusion or calendaring.

The third method is in situ grafting polymerization of macromolecular chains from the surface of the nanopowder. In the "grafting from" (Khaled 2009) or monomer functionalization technique; an initiator is used which can polymerize monomers in solution with the chains growing from the inorganic surface. The "grafting from" method is considered better than the "grafting to" method, as low molecular weight monomer molecules can diffuse rapidly to the nanoparticle surface, giving both higher graft densities and longer chain lengths. Hence dispersion of functionalized TiO_2 can potentially be enhanced using the grafting from method. Increasing the dispersion of TiO_2 nanoparticles in polymeric systems through functionalization can help decrease the size of agglomerates (Lott 2006). The nanoparticles will aggregate significantly in a lower polar medium if there is insufficient steric hindrance.

A common strategy for the surface functionalization of TiO_2 (and other oxides) is based on anchoring groups using chelating ligands that can carry additional functionalities that would allow the exploration of further applications of these materials. To achieve desirable properties

from nanomaterials, reactive organic groups can be attached to the surface of the inorganic nanocrystals. Significant work has been done to explore novel methods to prepare nanocrystalline rutile TiO_2 by controlling the size and morphology (Tahir 2006) as well as related properties.

Reinforcing polymers with inorganic oxides such as titanium dioxide is desirable and required for many emerging applications of interest such as bone cements. Nanoscale metal oxides such as TiO_2, SiO_2 are used as nanofillers but these oxides tend to agglomerate due to their large surface-area/volume ratios. Stable dispersions in various solvent systems can be prepared by providing adequate polymer functionality with evenly spaced metal oxide materials within the matrix of the polymer. The length of the polymer chains is known to affect the final spacing of the nanoparticles in the film, meaning that the stabilization of nanoparticles can be controlled by tuning the polymer chain length. However, to effectively coat a nanoparticle, the polymer chains must be attached to the surface by either physical or chemical means. This phenomenon is shown in Figure 1.3.

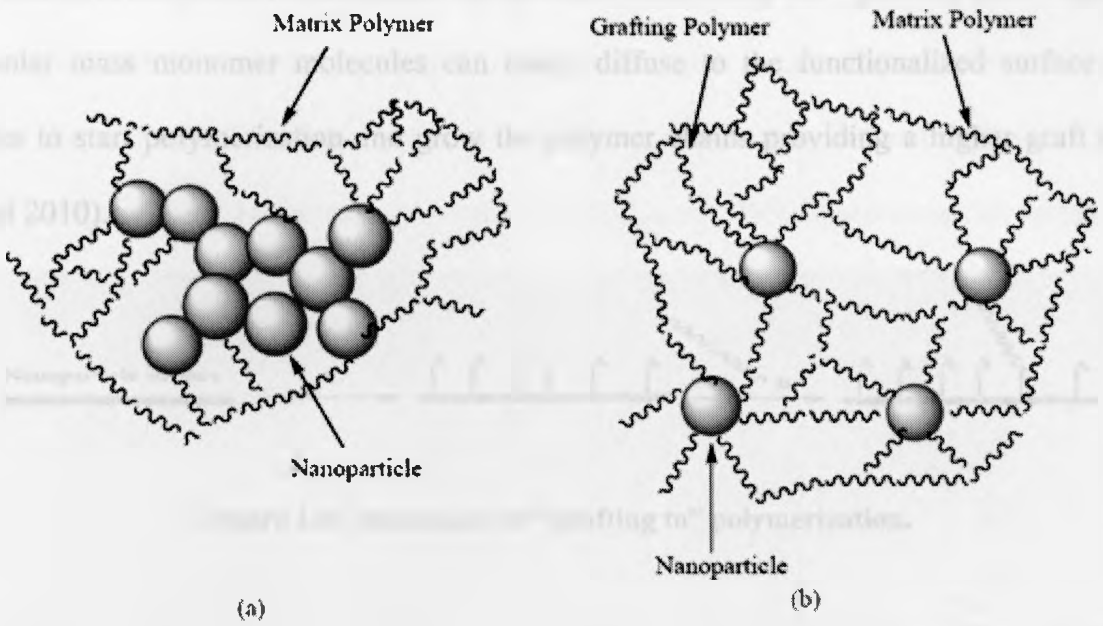

Figure 1.3: Schematics of: (a) agglomerated nano-particles in the matrix polymer in the case without grafting polymer and (b) separation of particles due to the grafting polymer. (Hojjati 2010).

To minimize the agglomeration of the nanoparticles and to enhance the filler-matrix interaction, many approaches have been examined including using a mechanical method (ultrasonic irradiation), or chemical method ("grafting to" and "grafting from") as mentioned earlier. Using the "grafting to" (Figure 1.4) approach, the number of polymer chains that one can graft to a surface is generally small, as the free volume occupied by each grafted polymer chain acts as a barrier to the attachment of subsequent chains. Hence, ''grafting to'' becomes increasingly difficult as more chains are added to the surface, limiting control of the molecular weight and polydispersity of the polymer chains. On the other hand, using the ''grafting from''(Figure 1.5) approach with initiators initially anchored to the nano surface allows higher graft density and better control of molecular weight and polydispersity of the polymer chains, as monomer molecules can easily diffuse to the particle surface. The "grafting to" polymerization approach is inherently limited in its ability to create high density grafted polymer as crowding of chains at

the surface prevents further attachment. On the other hand, using the ''grafting from'' approach, low molar mass monomer molecules can easily diffuse to the functionalized surface of the particles to start polymerization and grow the polymer chains providing a higher graft density (Hojjati 2010).

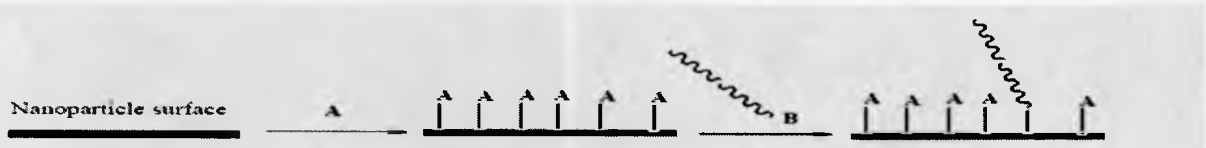

Figure 1.4: Mechanism of "grafting to" polymerization.

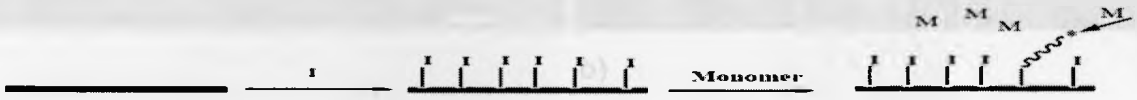

Figure 1.5: Mechanism of "grafting from" polymerization.

1.3. Need for Polymer Microspheres

Polymer particles in the size range of 1-100 microns are widely used in a diversity of applications for coatings, adhesives, toners, inks, paper, chromatography, bio-molecules, and PMMA bone cements containing DNA, proteins, and cells. For these applications, there is a tremendous need to be able to control the size and shape of the materials produced. To satisfy these requirements for morphology control, synthetic methods need to be developed to find an approach for efficient production. Microsphere polymer particles having uniform micron sizes could in principal be produced by several traditional polymerization approaches including emulsion, precipitation and dispersion polymerization, membrane emulsification, or multistage processes (Chang-Hyung et al. 2009). Figure 1.6 shows PMMA reinforced with functionalized and non functionalized TiO_2 composite prepared via bulk polymerization well dispersed PMMA

microspheres are observed in the matrix. As can be observed, PMMA reinforced with nonfunctionalized TiO_2 shows gaps and cracks in the polymer matrix (Figure 1.6b) while there is excellent dispersion of TiO_2 in the polymer matrix where the surface is functionalized (Khaled et al. 2007). (Figure 1.6a) The microspheres did not contain any TiO_2, motivating this research.

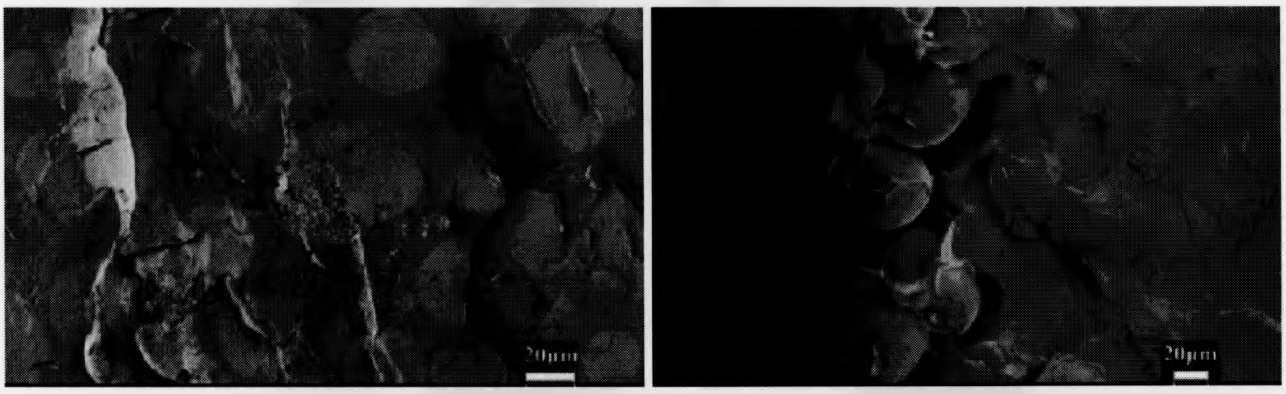

a) b)

Figure 1.6: SEM, PMMA reinforced with a) functionalized TiO_2 and b) nonfunctionalized TiO_2 composite.

Although these techniques can produce polymer beads, the results show a wide particle size distribution. Also these conventional methods are very material specific and time and labour consuming due to having several synthetic steps. Therefore, a useful synthetic method to prepare polymer microspheres, particularly with well dispersed oxide nanoparticles, is still a challenge. Figure 1.7 shows the size of naturally occurring microspheres.

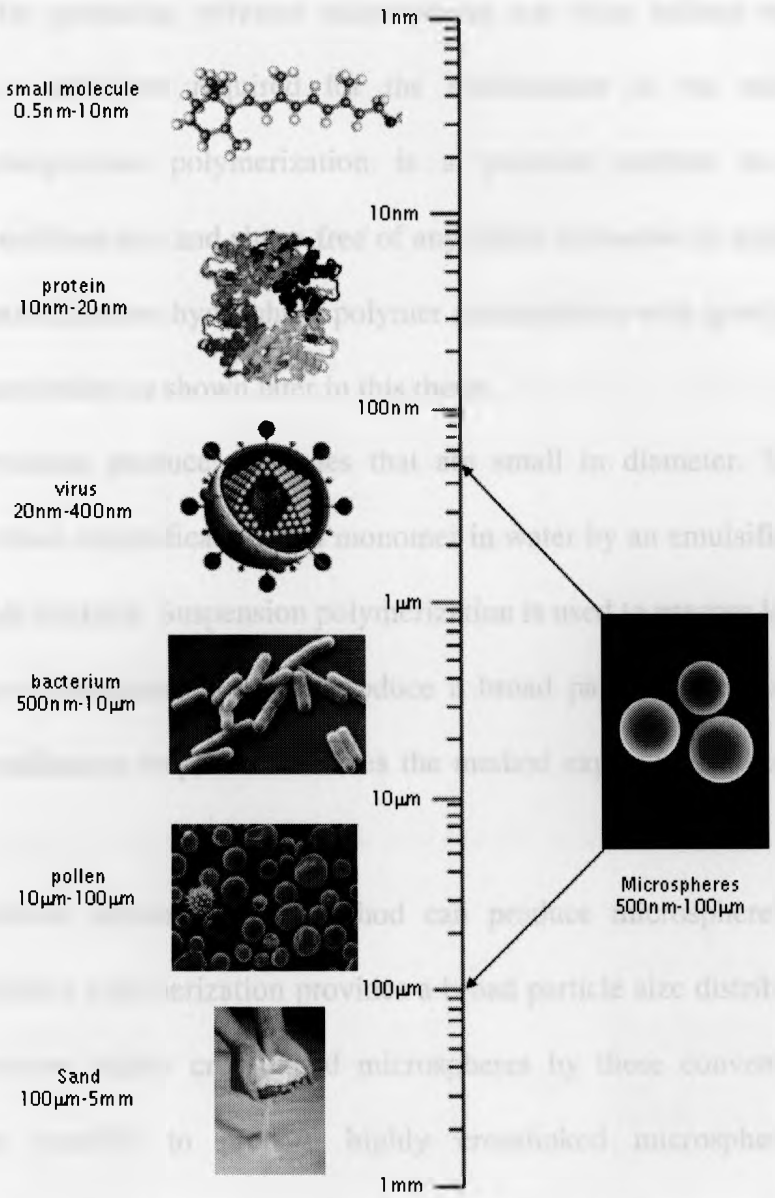

Figure 1.7: Nanometre and micrometer particles in nature.

1.3.1. Conventional polymerization approach and its limitation

Fully crosslinked polymer microspheres have been receiving considerable attention because of their improved thermal, chemical, and physical properties. However, the synthesis of such polymer colloids is difficult (Yang, Shim & Choe 2005). Conventionally, polymeric microspheres can be prepared by different well-known heterogeneous polymerization methods such as emulsion polymerization, suspension polymerization, and dispersion polymerization.

These techniques for preparing polymer microspheres are often tedious requiring removing added surfactant or stabilizer required for the stabilization of the microspheres during polymerization. Precipitation polymerization is a potential method to prepare polymer microspheres with uniform size and shape free of any added surfactant or stabilizer. However, it is difficult to get monodisperse hydrophilic polymer microspheres with good spherical shape by precipitation polymerization as shown later in this thesis.

Emulsion polymerization produces particles that are small in diameter. This heterogeneous polymerization involves emulsification of a monomer in water by an emulsifier and initiation by a water or oil-soluble initiator. Suspension polymerization is used to prepare large polymer beads with a wide range of diameters and will produce a broad particle size distribution and thus requires a size classification step, which makes the method expensive and causes low reaction yields.

Although the emulsion polymerization method can produce microspheres up to 1 mm in diameter and suspension polymerization provides a broad particle size distribution, it is difficult to obtain monodisperse highly crosslinked microspheres by these conventional methods. In addition, it's not possible to prepare highly crosslinked microspheres by dispersion polymerization. Precipitation polymerization has low yields for polymerization because the polymerized species consists of medium-soluble sol and insoluble gel parts. This may be due to the higher initiator and monomer concentrations required which would lead to the formation of precipitating large oligomeric species. Therefore, the desirable high yield could potentially be obtained by increasing the monomer and initiator concentrations in the precipitation polymerization.

Interfacial polymerization (Odian 2004) is similar to emulsion polymerization as it involves the dispersion of one liquid (e.g. oil) in another liquid (e.g. water) where the interface between the disperse phase and the continuous phase is very important. Interfacial polymerization is suitable for encapsulating liquids rather than solids as the penetration of reactants into the polymerization zone is much more easily accomplished from a liquid than a solid state. Interfacial polymerization is normally carried out at room temperature as high temperatures are not favourable to microsphere formation. Interfacial polymerization can be used to produce large microcapsules of around 20-30 microns diameter. Figure 1.8 shows a schematic drawing of interfacial polymerization (Huang, Kaner 2004). The presence of salts in the aqueous phase, a decrease in temperature and monomer concentration has been found to increase the microcapsule size (Quevedo, Steinbacher & McQuade 2005). However, interfacial polymerization, although attractive for microsphere formation, requires a new tunable continuous approach.

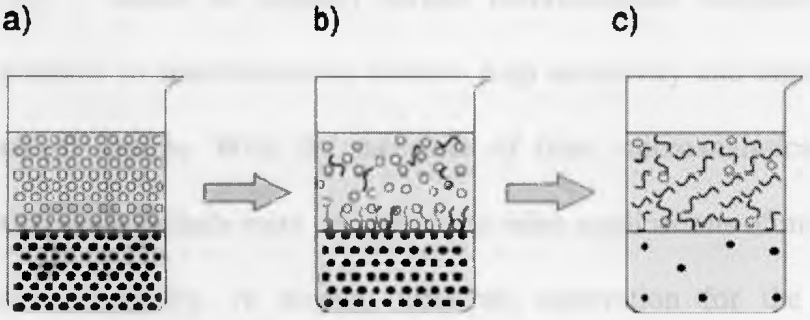

Figure 1.8: A schematic illustration of the synthesis of microspheres using interfacial polymerization, a) an interface is established between an organic phase (solid circles) and an aqueous phase (open circles), b) polymer spheres form at the interface, where the organic phase diffuses into the water phase and c) as the polymerization proceeds, microspheres accumulate in the aqueous phase.

1.4. Microfluidics

Microfluidics is an emerging technology which deals with the handling of fluids on the micron size scale. The application of microfluidics includes various diverse fields including chemical processing, food manufacturing, pharmaceutics, biotechnology and cosmetics. For the past several years these microfluidic devices have been used as new tools for controlling the formation of multi phase regimes of flow and potentially may be used to prepare spherical polymeric microparticles. The literature shows that microfluidics is an encouraging approach to the production of microparticles intended for cell encapsulation with this method having potential for tissue engineering applications such as bone cements (Baroud, Willaime 2004).

The field of microfluidics has four parents: molecular analysis, biodefence, molecular biology and microelectronics. The origins of microfluidics lie in micro analytical methods; i.e. gas-phase chromatography (GC), high-pressure liquid chromatography (HPLC) and capillary electrophoresis (CE) — which in capillary format revolutionized chemical analysis. These methods made it possible to simultaneously achieve high sensitivity and high resolution using very small amounts of sample. With the successes of these microanalytical methods, more compact and more versatile formats were developed for other applications of microscale methods in chemistry and biochemistry. A second, different, motivation for the development of microfluidic systems came with the realization that chemical and biological weapons posed major military and terrorist threats. To counter these threats, the Defence Advanced Research Projects Agency (DARPA) of the US Department of Defence supported a series of programs in the 1990s aimed at developing field-deployable microfluidic systems designed to serve as detectors for chemical and biological threats. These programs were the main stimulus for the rapid growth of academic microfluidic technology. The third motivational force came from the field of molecular biology, particularly from the explosion of interest in genomics in the 1980s,

followed by the advent of other areas of microanalysis related to molecular biology. These included high-throughput DNA sequencing, required analytical methods with much greater throughput, and higher sensitivity and resolution than had previously been contemplated in biology. The fourth contribution was from microelectronics. The original hope of microfluidics was that photolithography and associated technologies that had been so successful in silicon microelectronics, and in microelectromechanical systems (MEMS), would be directly applicable to microfluidic approaches. Neither glass nor silicon has all the properties (especially permeability to gases) required for work with living mammalian cells (Whitesides 2006).

Interest in the use of continuous flow micro-reactor technology in the pharmaceutical and fine chemicals industries continues to grow. With the potential for lower operational costs and enhanced process safety, the application of this technology at an early R&D stage and for making polymers is only beginning to be recognized. The use of continuous flow micro-reactors can potentially facilitate the scale-up of established procedures for continuous processing and circumvent time-consuming synthetic protocols. The implementation of micro-flow devices for high throughput synthesis can potentially also have a significant impact on polymerization processes, as the polymer synthesis can be performed in very short reaction times and with very small amounts of material controlling polymer bead size. Overall, the time to market can be drastically shortened, rendering the entire process cycle more economical and efficient.

Microfluidics is a field dedicated to miniaturized plumbing and fluid manipulation. A wide variety of physical phenomena occurs in microfluidic devices, which is essentially an area of research drawn from classical physics and chemistry-fluid mechanics, including electrostatics, thermodynamics, statistical mechanics, elasticity, and polymer physics. Figure 1.9 shows a

miniaturized microfluidics device (Micronit Microfluidics) used for examining flow chemistry in droplet formation by researchers at the University of Michigan.

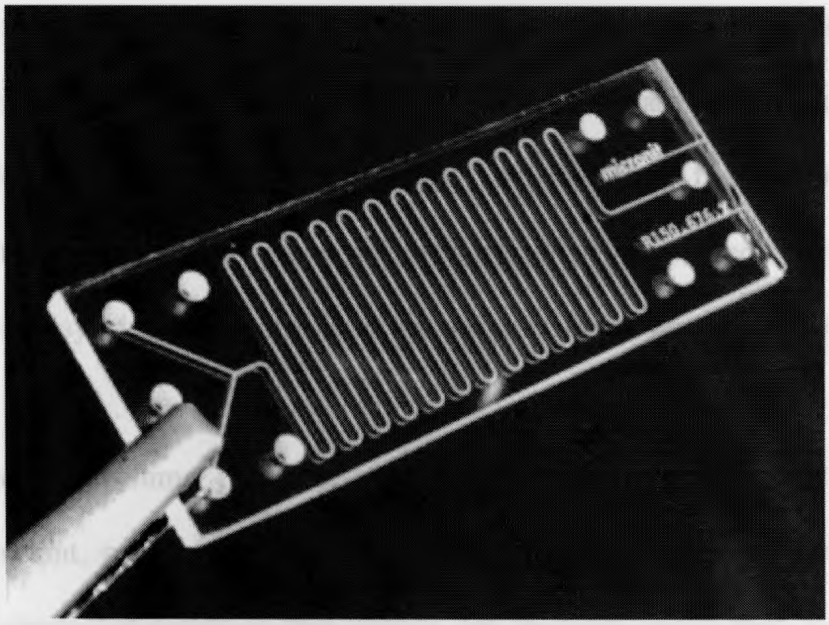

Figure 1.9: Miniaturized microfluidics device. (Webb 2009).

To explain these multi-scale phenomenons, dimensionless numbers are being utilized, i.e. the Reynolds number Re which relates inertial forces to viscous forces; Peclet number Pe which relates convection to diffusion; and the capillary number Ca which relates viscous forces to surface tension. The Reynolds number, Peclet number, and Capillary number are used to determine the type and behaviour of the flow.

It should also be mentioned that in the case of microfluidic devices, inertial forces are small compared to viscous forces. Mixing taking place in any system (whether in turbulent or laminar flows) ultimately occurs due to molecular diffusion. Purely diffusive mixing can be desirable or not, depending on the application. Microfluidic chemical reactors require different solutions to be brought together and mixed rapidly, allowing the dynamics of the reactions to be probed. However it should be noted that the faster the mixing, the harder the separation. Hence,

controlling dispersion in microfluidic devices is very important. When fluid elements move chaotically, they are stretched and folded exponentially, enhancing mixing.

The Capillary number Ca is a dimensionless number associated with a liquid that compares the intensity of liquid viscosity and surface tension. Miscible fluids are assumed to flow in parallel streams alongside one another, with tracers being able to diffuse freely from one stream to another. Between immiscible fluids, however, the surface tension γ affects the dynamics of the free surface which plays an important role in microfluidic flows when immiscible free surfaces are present.

The large surface to volume ratios of microfluidic devices renders any surface effects increasingly important, particularly when free fluid surfaces are present. Surface tension can exert significant stress that results in free surface deformations and/or bulk liquid motion. The use of the Reynolds number in a microfluidics system allows studying the dynamics of individual polymer molecules in precisely defined flows. A central goal of most research in complex fluids involves relating macro-scale behaviour to micro-scale structure, and microfluidic devices show considerable potential towards this end (Whitesides 2006).

Droplets of different sizes and size distributions are created based on different geometrical techniques (Link et al. 2004). In microfluidics, a T-junction microchannel is one of the most frequently used configurations for droplet formation and manipulation. T-junction geometry is widely used due to its ease of droplet formation and uniformity of the formed droplets (Nisisako, Torii & Higuchi 2002). The droplet size increases while increasing the pressure of the dispersed phase and there is also a decrease in the size when there is an increase in the pressure of the continuous phase. The droplet formation phenomenon at the T-junction microchannel can also be controlled by various parameters; flowrates, viscosities, the interfacial tensions as well as the

channel geometry (Graaf et al. 2006) as will be examined in this thesis. Nano-fluids (such as containing TiO_2) have been found to exhibit different thermo-physical and interfacial properties such as thermal conductivity, viscosity, and surface tension as compared to their base fluids (Mursheda, Leong & Yanga 2008). Apart from the enhanced thermo-physical and interfacial properties of the nano-fluid, this fluid is suitable for use in microfluidics because they contain nanoparticles, which are orders of magnitude smaller than the microfluidic devices themselves (Murshed et al. 2009).

Interfacial tension of the nanoparticles are smaller and decrease more rapidly with temperature as nanoparticles experience Brownian motion and interact with the liquid molecules resulting in a reduced cohesive energy at the interface. An elevated temperature intensifies the Brownian motion lowering the cohesive energy and reduces the surface or interfacial tension.

Over the last two decades, there has been an extensive growth for the design and fabrication of microfluidics devices and systems for biological and medical applications (Wang, Zhao & Pan 2009). An emerging technique, Lab-on-a-chip (LOC) focuses precisely on handling a very tiny volume of fluid and it plays an essential role in modern analytical chemistry and biomedical studies. Although, a great deal of LOC devices have been demonstrated by a conventional micro-fabrication techniques with high reliability and ultrafine resolution, these devices have to overcome a very crucial obstacle, the need for expensive equipment, the extensive usage of clean-rooms as well as a lengthy processing cycle and the chance of blockage in the system. Understanding the advantages and disadvantages of the microfluidics system allows designing a more suitable system for the polymerization process. This approach is taken into consideration for the design of the experimentally used microfluidic setup as explained in chapter 3.

Polymerizations carried out with microfluidics offer several potential advantages over the conventional polymerization methods, giving more uniform size and shape polymer microspheres. The phases in the microfluidics system are called the continuous phase (aqueous phase) and the droplet phase (dispersed phase), with the chemical nature of the latter phase determining the transformation of droplets into microparticles. Polymerizing the droplets can then be carried out by thermal initiation (Sugiura et al. 2002)or UV-initiation (Nisisako, Torii & Higuchi 2004). Droplets of the dispersed polymer phase can be hardened by different methods such as solvent evaporation (Seo et al. 2005), chemical reaction (Cohen et al. 2001), or ionic cross-linking (Keng-Shiang, Tzung-Heng & Yu-Cheng 2006). Oil-in-water or water-in-oil emulsions carried out in microfluidics have been captured by coascervation (Nakagawaa et al. 2004), by photoinitiated polymerization to create solid beads (Nisisako, Torii & Higuchi 2004), by a double emulsion method to create hollow capsules (Utada et al. 2005)or by interfacial polymerization (Takeuchi et al. 2005). All three mentioned methods use a two-step procedure where the droplet is first produced at a fluid junction and then polymerized downstream (Quevedo, Steinbacher & McQuade 2005).

1.5. Outline of Thesis

In this thesis, functionalization of the surface of TiO_2 (titanium dioxide) is examined using the following functionalizing agents: methacrylic acid, 2-carboxyethyl acrylate and 10-undecenoic acid. The functionalizing procedure is carried out at various pH values with the optimized value used for the modification of the surface of TiO_2. The polymerization of MMA is subsequently carried out using traditional precipitation polymerization reinforced with the functionalized n-TiO_2, and microfluidics using interfacial polymerization. A novel microfluidics system is

designed using CFD (computational fluid dynamics) modelling and an experimental approach of the microfluidics T-junction for the purpose of polymerization of methyl methacrylate (MMA). The advantages and limitations of the microfluidics design over the conventional precipitation polymerization are compared and discussed. The results obtained are analysed by using several analysis methods such as TGA, FTIR, GPC, SEM, TEM, RAMAN, and Light microscopy.

The flow behaviour and pattern of the dispersed phase and the continuous phase engaged in the Micro TEE system is designed and discussed with the CFD (computational fluid dynamics) modeling based on the geometry of the T-junction.

CHAPTER 2: FUNCTIONALIZATION AND CHARACTERIZATION OF NANO TITANIA (n-TiO_2) cement

2.1. Introduction

The field of polymer composites is transforming from using traditional fillers (e.g. carbon fibers) to nanoscale fillers that add unique and multifunctional properties to the polymer matrix. Nanoparticles have high surface area to volume ratios and at low wt %'s nanoparticles have the potential to drastically transform the properties of the host polymer matrix (Hamming et al. 2009).

For use in emerging applications, especially those using hydrophobic organic solvents, the surface of hydrophilic TiO_2 nanoparticles needs to be modified by organic modifiers. The main approach to modify the surface of titanium dioxide is; *in situ* or postmodification. For *in situ* modification, the attachment of modifier molecules onto the TiO_2 nanoparticles is ceased during the growth of the nanocrystals. It is difficult to have a synthesis method that can maintain good control over the growth features as well as the surface chemistry of the nanocrystals. In many applications, a specific morphology, well defined particle size, and shape are required. A useful strategy is to modify the surface of TiO_2 with modifier molecules by postmodification.

To achieve desirable properties from the nanoparticles, reactive organic groups need to be attached to the surface of the inorganic nanocrystals. Carboxylic acids are often used as such modifiers, with coordination of the carboxylic groups (COOH) to the top surface Ti atoms (Qiyun et al. 2010). Usually, the postmodification method immerses TiO_2 particles and films into an organic solution to absorb the carboxylic modifier at room temperature or by ligand exchange reactions. The conventional postmodification by immersion method normally leads to a weak and unstable binding of modifier to the TiO_2 surface, which results in desorption of the modifier during application. However Ti (IV) is well known to be able to form carboxylate complexes. In

these complexes, the acetate can potentially coordinate with the metal as a chelating, bridging bidentate or monodentate formation. Figure 2.1 shows that a carboxylic group can form coordination bonding with TiO_2 in several ways; carboxylate is bound to one Ti^{IV} center in a chelating bidentate mode. It can also be bound to one Ti^{IV} in a monodentate (ester-like linkage) mode and the carboxylate group could bind with each of its oxygen atoms to a Ti^{IV} center of the surface yielding the bridging bidentate mode. The carboxylic ions adsorb in a dissociative process with the two oxygen atoms bonding to the surface titanium ions, with the proton (H^+) bonding to the bridging oxygen ions. Figure 2.1 shows the possible binding modes of carboxyl group on TiO_2 nanoparticles. The carboxylate can bind to one Ti^{IV} in a monodentate (ester-like linkage) mode (iv). The carboxyl group can also bind with each of its oxygen atoms to a Ti^{IV}(Khaled 2009) center of the surface yielding the bridging oxygen ions (v). And finally, the carboxylate is bound to one Ti^{IV} center in a chelating bidentate mode (vi).

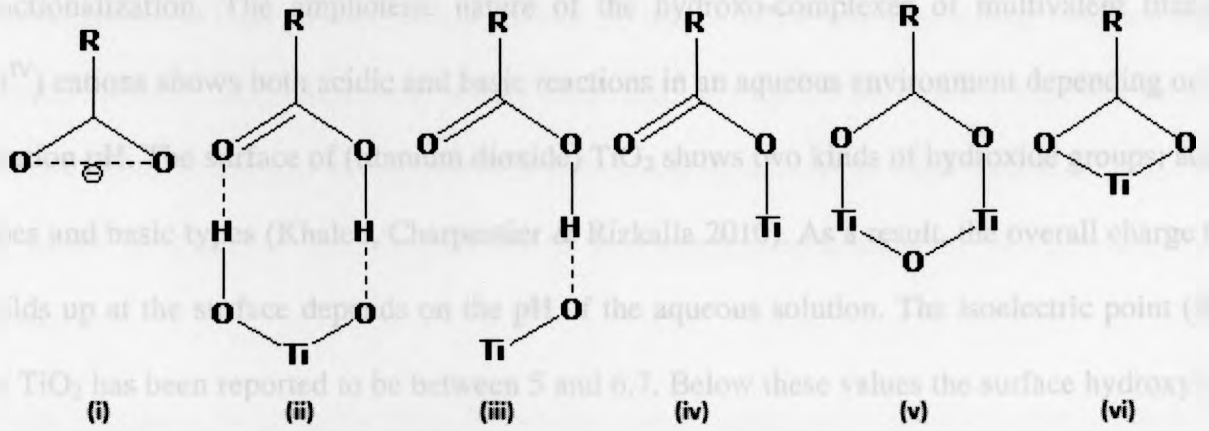

Figure 2.1: Possible Binding Modes of COOH Group on TiO_2 nanoparticles (i) Electrostatic Attraction, (ii, iii) H-Bonding, (iv) Monodentate(Ester-like Linkage), (v) Bidentate Bridging, and (vi) Bidentate Chelating.

Although the presence of multi carboxylic groups increases the reaction between the monomer and TiO_2, an anhydrous solvent has to be used, as traces of water in the solvent will break the weak interaction ester-like linkages formed by adsorption during the immersion process (Wade 2010). Moreover, the difficulties in getting well dispersed nanocrystals and/or in filling efficiently the pores of nanosized aggregates limits the control of the surface coverage in the modification by immersion or ligand exchange reactions. Hence, the approach to bind the carboxylic acid molecules with a stable chemical interaction on TiO_2 nanoparticles by post-modification remains a scientific challenge. In particular, a method that takes advantages of binding organic modifiers on the particles without changing their original growth features in a controllable manner would be useful (Dobson, McQuillan 2000) by adjusting the surface coverage of modifier (Qiyun et al. 2010).

The surface charge of n-TiO_2 powders can be controlled by adjusting the pH of the medium for functionalization. The amphoteric nature of the hydroxo-complexes of multivalent titanium (Ti^{IV}) cations shows both acidic and basic reactions in an aqueous environment depending on the solution pH. The surface of (titanium dioxide) TiO_2 shows two kinds of hydroxide groups; acidic types and basic types (Khaled, Charpentier & Rizkalla 2010). As a result, the overall charge that builds up at the surface depends on the pH of the aqueous solution. The isoelectric point (IEP) for TiO_2 has been reported to be between 5 and 6.7. Below these values the surface hydroxyl ion is fairly positive to bind negative carboxyl ions of the bifunctional monomer.

$$Ti\text{-}OH + H_2O \rightarrow [Ti\text{-}O]^- + H_3O^+ \quad \text{(Basic reaction)}$$

$$Ti\text{-}OH + H_2O \rightarrow [Ti\text{-}OH_2]^+ + OH^- \quad \text{(Acidic reaction)}$$

Thus the functionalization at different pH values results in different extents of functionalization. Functionalization provides organophilicity to the n-TiO_2 powders, which can result in stronger

adhesion of the nanopowders to a polymer matrix. The COOH group of the carboxylic acid can protonate at low pH, and it's interesting to note that the COOH group may be deprotonated into carboxylate anions (COO^-) and Ti-OH into Ti-O^- in basic conditions as well (Qiyun et al. 2010). Scheme 1(Pasqui et al. 2007)shows the reaction taking place when TiO_2 reacts with a carboxylic group present on a functionalizing agent.

()()

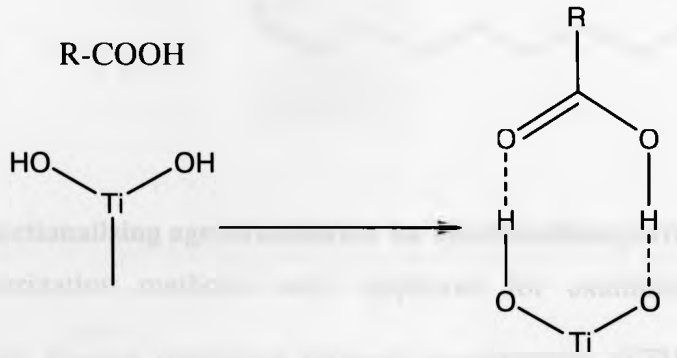

Scheme 1: Reaction of TiO_2 and carboxyl group.

Functionalized n-TiO_2 powder is organophilic in nature and it provides strong adhesion to the polymer matrix which allows only a very small amount of water absorption. It should be noted that at a higher loading of n-TiO_2 powders there is a large amount of water uptake. This is due to the spatial proximity of the nanopowders, as well as agglomeration of the nanopowders within the matrix.

Figure 2.2 shows the structure of the three bifunctional monomers examined in this research. The carboxyl group of the coupling agent methacrylic acid (MA) attaches to the surface of the n-TiO_2 powders by carboxylic coordination with the Ti ions and by electrostatic bonding with the surface OH^+ which predominates in acidic solution.

Methacrylic Acid

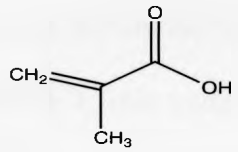

2-Carboxyethyl Acrylate

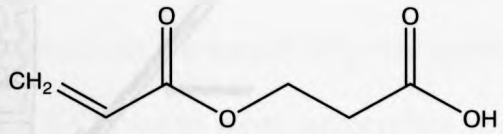

10-Undecenoic Acid

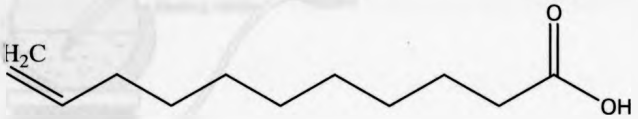

Figure 2.2: Functionalizing agents employed for functionalizing surface of n-TiO_2.

A variety of characterization methods were employed for examining the functionalized nanomaterials including Fourier transform infrared spectroscopy (FTIR), thermogravimetric analysis (TGA), RAMAN spectroscopy and dynamic light scattering (DLS).

2.2) Experimental set up: materials and methods

2.2.1) Materials

Commercial Titanium(IV) oxide, mixture of nanopowder < 100 nm (BET), 99.5 % trace metal basis (Sigma-Aldrich), methacrylic acid MA (99.99%, Sigma-Aldrich) 2-carboxyethyl acrylate (99.99%, Sigma-Aldrich) and 10-undecenoic acid (99.99%, Sigma-Aldrich), 2 propanol anhydrous (99.99% Sigma-Aldrich), AIBN (2,2′-Azobis(2-methylpropionitrile)) (Toronto research company), KOH potassium hydroxide (VWR) were all used as received.

2.2.2. Functionalization setup

The functionalization reactions were carried out in a 250 mL three-neck round bottom flask fitted with reflux condenser and thermometer. The reactor was heated by a heating mantle (Glas-Col 1662868) controlled by a voltage regulator (Powerstat 3PN116C) (Figure 2.3).

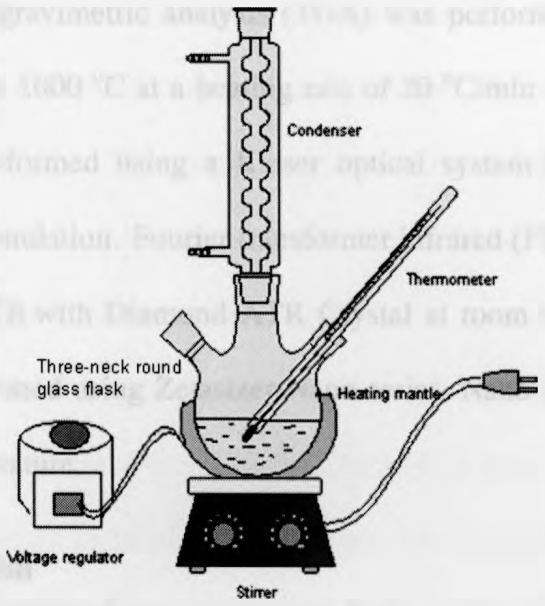

Figure 2.3: Schematic of experimental setup for functionalization of titania nanopowders.

2.2.3. Functionalization procedure

The commercial TiO_2 nanopowders were calcined at 500°C for 16 hours to impart crystallinity and thermodynamic stability (Khaled 2009). Several bifunctional agents were investigated including methacrylic acid, 2-carboxyethyl acrylate and 10-undecenoid acid (Figure 2.2). 0.1g of the calcined TiO_2 powder was dispersed in 35 mL of 2-propanol anhydrous for 1 hour with the aid of ultrasonic agitation, followed by reacting with 3 mL of functionalizing agent at 80 °C for 24 hours with constant stirring of 300 RPM and under argon gas. Several different values of pH ranging from 3.5 to 6.75 were examined to find the most suitable pH for the functionalization reaction. In order to increase the pH of the solution, a few drops of potassium hydroxide (KOH) were added to the reaction mixture. The pH of the reaction medium was measured using pH meter (HANNA instrument HI83141 pH/mV/^{o}C). The reaction product was then centrifuged and washed, and dried at 80 °C in a vacuum oven overnight. The experiments were repeated a number of times with MA, 2-carboxyethyl acrylate and 10-undecenoic acid.

Characterization: Thermogravimetric analysis (TGA) was performed using a Mettler-Toledo TGA/SDTA851^e from 25 to 1000 ^oC at a heating rate of 20 ^oC/min under nitrogen atmosphere. RAMAN analysis was performed using a Kaiser optical system (RXN1-785) with 5 times exposure and 20 times accumulation. Fourier transformer infrared (FTIR) was performed using a Thermo Scientific Smart iTR with Diamond ATR Crystal at room temperature. Dynamic light scattering (DLS) was performed using Zetasizer Nano series, Nano S model ZEN 1600 particle size analyser at room temperature.

2.3. Results and discussion

The challenge for preparing polymer nanocomposites is the agglomeration of the nano fillers in a polymer matrix which leads to poor performance of the composite. To avoid the nanophase agglomeration when it is blended with the polymer matrix, three bifunctional monomers as shown in Figure 2.2 are examined in this chapter that can chemically link the TiO_2 nanomaterials to a polymer matrix. These molecules were examined by TGA, FTIR, RAMAN & partitioning studies that can modify the surface of titania using a Ti-carboxylic coordination bond, with a subsequent vinyl group for polymerization.

2.3.1. TGA

Thermogravimetric analysis or TGA was performed to measure changes in weight in relation to a change in temperature. TGA is commonly employed to determine the degradation temperatures, absorbed moisture content of materials, the level of inorganic and organic components in materials and solvent residues. Figure 2.4 shows the thermal weight loss of both nonfunctionalized and functionalized n-TiO_2 powders reacted with the three examined bifunctional monomers. As expected, the calcined TiO_2 did not show any significant weight loss (<1%), whereas the functionalized TiO_2 with the functionalizing agents show substantial weight loss. The weight loss in the temperature range of 0-200^oC is due to any adsorbed solvent present

on the surface of n-TiO_2 as well as any unreacted bifunctional monomer. The boiling points for the bifunctional monomers, methacrylic acid, 2-carboxyethyl acrylate, 10-undecenoic acid are 161, 103, and 137 °C respectively. The weight loss observed at or below 200 °C is mainly due to evaporation of solvent or possible uncoordinated materials in the samples of Ti-methacrylic acid, Ti-2-carboxyethyl acrylate and Ti-10-undecenoic acid.

The weight loss from 200-400 °C is attributed to the breakage of chemical bonds formed between the TiO_2 and carboxylic acid (Khaled et al. 2007). The weight loss in this range shows there is strong chemical bonding present, indicating TiO_2 surface functionalization. An enhanced thermal stability of the functionalized titania nanopowders was observed compared to the calcined nanopowders using TGA. The second step from 200-400 °C shows there is a chemical bond formed between the TiO_2 and 2-carboxyethylacrylate. A similar trend is observed when TiO_2 is functionalized with methacrylic acid and 10-undecenoic acid. The greater weight loss observed in the case of 2-carboxyethyl acrylate and methacrylic acid suggests that more organic bifunctional monomer was grafted to the surface of the TiO_2, giving a functionalization reaction.

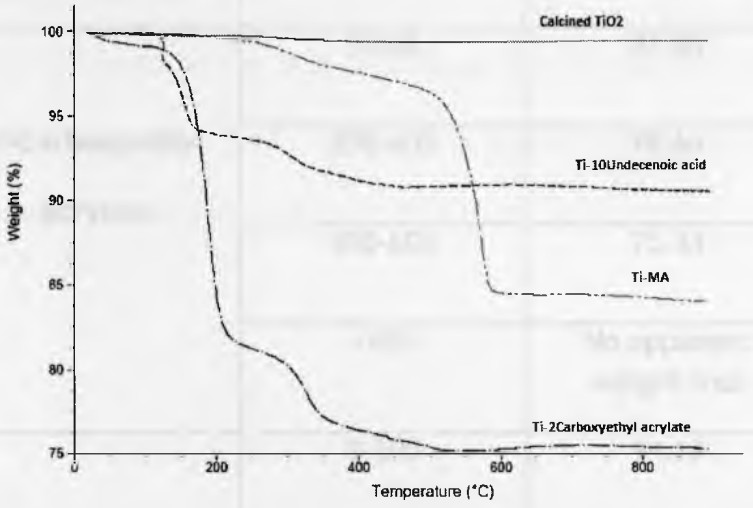

Figures 2.4: TGA curves of the 2 wt% nonfunctionalized and functionalized TiO_2, Ti-methacrylic acid, Ti-2-carboxyethyl acrylate and Ti-10undecenoic acid at 65°C in 2-propanol.

An increase in the weight loss observed in the TGA graph corresponds to an increased amount of bonded carboxylic groups co-ordinated to the titania surface. The weight loss observed with respect to temperature for each functionalized TiO_2 with bifunctional monomer is shown in Table 2.1. The most weight loss is observed when TiO_2 was functionalized with: 2-carboxyethyl acrylate, methacrylic acid and 10-undecenoic acid respectively at 400-600 ^{o}C temperature range. There was no apparent weight loss observed at >600 ^{o}C.

Table 2.1: TGA result shows the weight % with respect to temperature.

Bifunctional monomer	Temperature(°C)	Weight (%)
Methacrylic Acid	0-200	98
	200-400	97.64
	400-600	85.81
	>600	No apparent weight loss
2-Carboxyethyl acrylate	0-200	83.86
	200-400	78.64
	400-600	75.34
	>600	No apparent weight loss
	0-200	94.18
	200-400	93.35

10-Undecenoic Acid	400-600	90.78
	>600	No apparent weight loss

The effect of pH on functionalization of the surface of titanium dioxide was examined in order to optimize co-ordination. The weight loss occurred with varying the pH of the medium from 3.83 to 5.5 and 6.7 as shown in Figure 2.5. Most functionalization was observed when the pH of the medium was close to 5.5 for the three functionalizing agents. As was mentioned earlier, the isoeletric point (IEP) for TiO_2 is between 5 and 6.7.

To enhance the adsorption of the carboxylic group of methacrylic acid on the titania surface, the pH of the reaction medium was adjusted by adding a few drops of potassium hydroxide (KOH). The observed increase in the pH of the media results in dissociation of the carboxylic ions of the methacrylic acid (Hirata et al. 1992). This may partly be due to the negative charge on the n-TiO_2 powders over the IEP and partly caused by the reaction of carboxylic ions with K^+ ions from potassium hydroxide (KOH).

Figure 2.5 and Table 2.2 shows the TGA results when titanium dioxide is functionalized with methacrylic acid at pH values of 3.7, 5.5, and 6.2. It is apparent that the most suitable pH value for the functionalization of the surface of TiO_2 is 5.5 (Khaled et al. 2007).

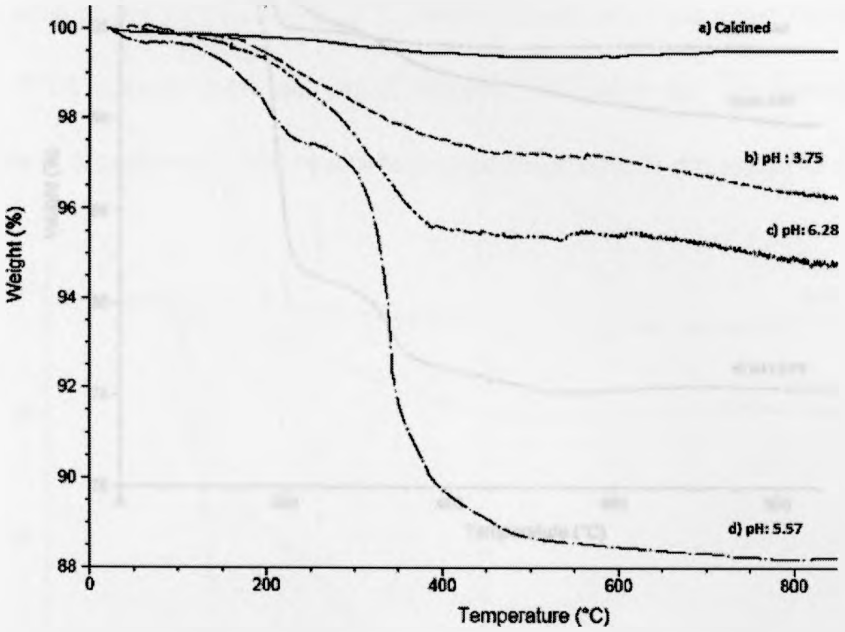

Figure 2.5: TGA graph of functionalized titanium dioxide with methacrylic acid at pH of b) 3.7, c) 6.2, d) 5.5 and a) calcined titanium dioxide.

Table 2.2: Weight loss with respect to temperature at different pH values for functionalized TiO_2 with methacrylic acid.

pH	Temperature Range(°C)	Weight (%)
3.7	200-400	95.58
5.5	200-400	97.51
	400-600	88.70
6.2	200-400	95.58

Figure 2.6 and Table 2.3 represents the TGA results when TiO_2 is functionalized with 2-carboxyethyl acrylate at pH values of 5.7, 5.8, and 6.8. The initial pH value of the medium is 5.7 in the reaction vessel with this pH value being the most suitable for the functionalization of the surface of titanium dioxide with 2-carboxyethyl acrylate bifunctional monomer.

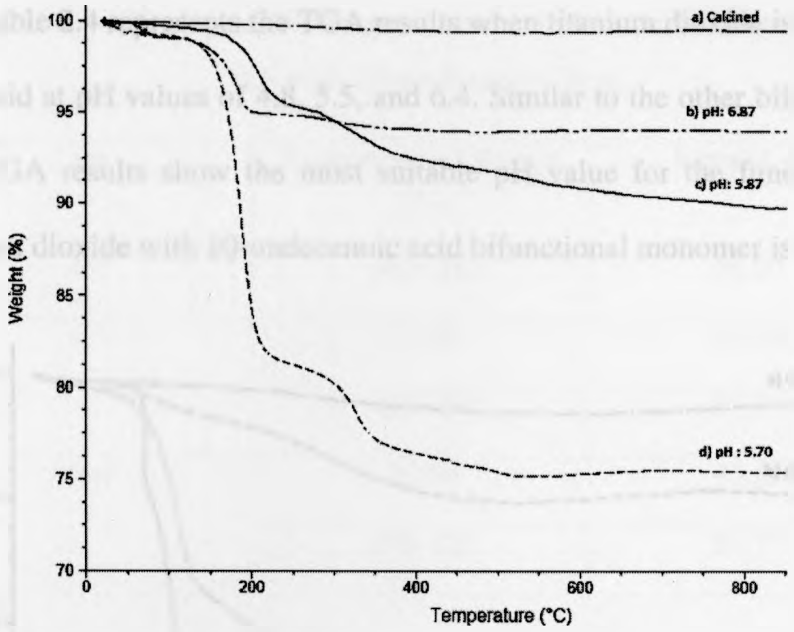

Figure 2.6: TGA graph of functionalized titanium dioxide with 2-carboxyethyl acrylate at pH of b) 6.8, c) 5.8, d) 5.7 and a) calcined titanium dioxide.

Table 2.3: Weight loss with respect to temperature at different pH values for functionalized TiO_2 with 2-carboxyethyl acrylate.

pH	Temperature Range (°C)	Weight (%)
5.7	0-200	81.89
	200-400	77.00
5.8	0-200	95.02
6.8	0-200	95.76
	400-600	92.60

Figure 2.7 and Table 2.4 represents the TGA results when titanium dioxide is functionalized with 10-undecenoic acid at pH values of 4.8, 5.5, and 6.4. Similar to the other bifunctional molecules examined, the TGA results show the most suitable pH value for the functionalization of the surface of titanium dioxide with 10-undecenoic acid bifunctional monomer is 5.5.

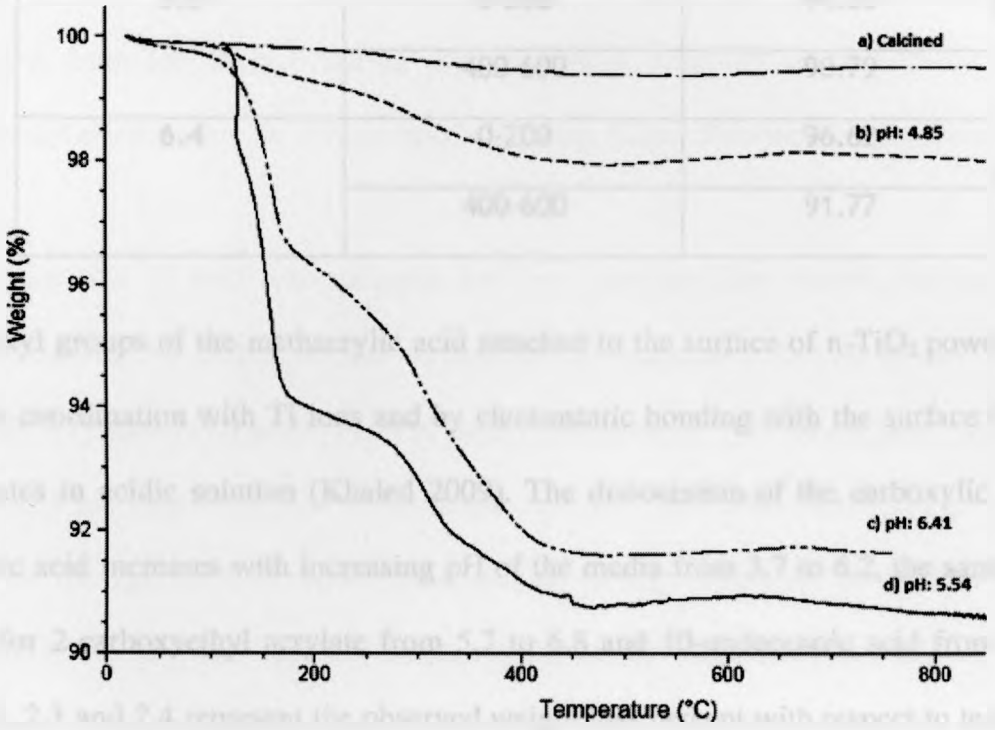

Figure 2.7: TGA graph of functionalized titanium dioxide with 10-undecenoic acid at pH of b) 4.8, c) 6.4, d) 5.5 and a) calcined titanium dioxide.

Table 2.4: Weight loss with respect to temperature at different pH values for functionalized TiO_2 with 10-undecenoic acid

pH	Temperature Range (°C)	Weight (%)
4.8	400-600	98.09
5.5	0-200	94.20
	400-600	90.79
6.4	0-200	96.62
	400-600	91.77

The carboxyl groups of the methacrylic acid attached to the surface of n-TiO_2 powders both by carboxylic coordination with Ti ions and by electrostatic bonding with the surface OH^+, which predominates in acidic solution (Khaled 2009). The dissociation of the carboxylic ions of the methacrylic acid increases with increasing pH of the media from 3.7 to 6.2, the same trend was observed for 2-carboxyethyl acrylate from 5.7 to 6.8 and 10-undecenoic acid from 4.8 to 6.4. Tables 2.2, 2.3 and 2.4 represent the observed weight loss percent with respect to temperature at several pH values for methacrylic acid, 2-carboxyethyl acrylate and 10-undecenoic acid respectively. Figure 2.5, 2.6, 2.7 show the TGA graphs of titanium dioxide functionalized with methacrylic acid, 2-carboxyethyl acrylate, 10-undecenoic acid respectively. Increasing the pH by adding a few drops of KOH closer to pH 7 in all the three bifunctional monomer reactions with titanium dioxide decreases the extent of functionalization. This might be due to the negative surface charge on n-TiO_2 powders (Khaled 2009) over the IEP (Hirata et al. 1992) and also due to the reaction between the carboxylate ions with K^+ ion from the KOH drops added to adjust the pH is the three neck round bottom. The pH values in the range of 5.5 to 5.7 were found to show the most weight loss observed with respect to temperature. Hence, it can be concluded that the

functionalization reactions taking place at these pH values provides maximum extents of functionalization among the different pH values examined for all three functionalizing agents. This may be attributed to the optimum combination of the surface charge on titania and the amount of dissociated carboxylate ions in solution. It should be noted that the increase in the extent of functionalization on the n-TiO_2 powders will allow a higher number of polymer chains to be grown from the surface during polymerization, resulting in an increase in thermal degradation temperature for the nanocomposite(Huang, Kaner 2004)as shown in chapter 3.

2.3.2. FTIR

The FTIR spectra of both the calcined and the functionalized titania nanopowders with methacrylic acid (MA), 2-carboxyethyl acrylate and 10-undecenoic acid are shown in Figure 2.8. In Figure 2.8 (a) there is no peak observed from 1300-1800 cm^{-1} on the calcined TiO_2 indicating the absence of any organic groups on the titania surface. The band at 1630 cm^{-1}, 1680 $cm^{-1}$and 1543cm^{-1} on the spectra b-d) shows the existence of the vinyl bond of 10-undecenoic acid, methacrylic acid and 2-carboxyethyl acrylate respectively while the small band at 1240 cm^{-1} corresponds to a CH_3 group. The band at 1700 cm^{-1}, 1680 cm^{-1}, 1710 cm^{-1} on the spectra (b), (c) and (d) respectively corresponds to the C=O bonds of very small amounts of carboxylic acid residue. FTIR is an established technique for analyzing the complexes of metal carboxylate species (Khaled et al. 2007). The peaks at 1410, 1440 cm^{-1} on spectrum (b) and peaks 1400, 1430 and 1543 cm^{-1}observed in spectrum (d) in Figure 2.8 represent the bond formation for Ti-acetate (Khaled et al. 2007).The IR spectrum shown in Figure 2.8 (b, c, d) confirms that the carboxyl group of 10-undecenoic acid, methacrylic acid and 2-carboxyethyl acrylate, has been coordinated to the titania surface. As a result, titania is functionalized with carboxyl group and the vinyl group present on the structure can be employed for subsequent polymerization with unsaturated monomer during the synthesis of polymer-titania nanocomposites.

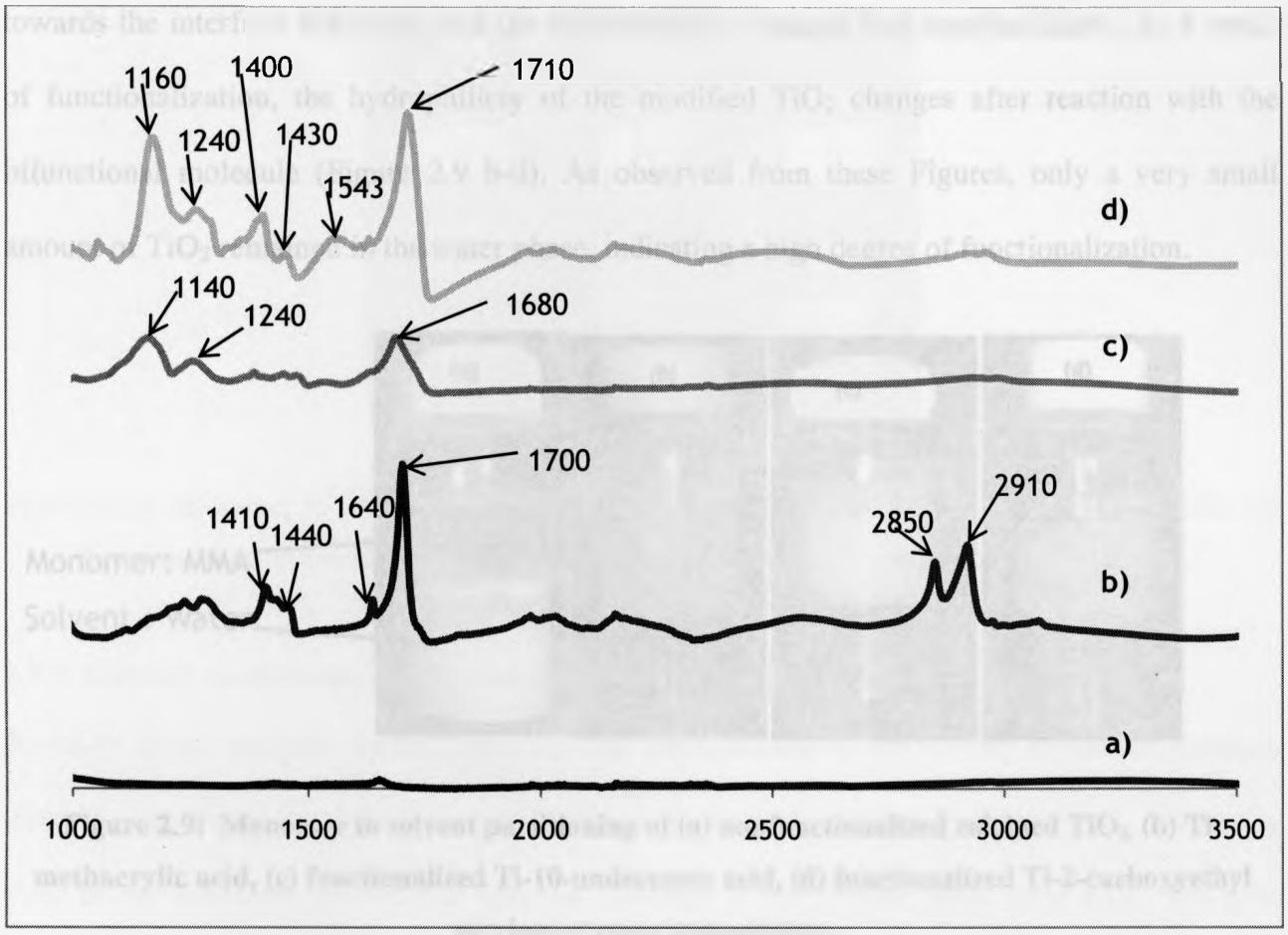

Figure 2.8: FTIR Spectra of a) calcined n-TiO_2 powders, b) functionalized with 10-Undecenoic acid c) Methacrylic acid and d) 2-Carboxyethyl acrylate.

2.3.3. Monomer solvent partitioning

Before functionalization, n-TiO_2 is hydrophilic. After the coordination of the functionalizing agents to its surface, TiO_2 is less hydrophilic and more hydrophobic with additional co-ordination. The vinyl group CH_2=CH- of the acrylate group and the H^+ on the bridging oxygen atom of the surface of titania contributes to the organo- and hydrophilicity respectively. Figure 2.9 shows the dispersion of the n-TiO_2 in layers of MMA and water at room temperature. The nonfunctionalized n-TiO_2 is well dispersed in the water phase as shown in (a), while the functionalized n-TiO_2 exhibited good dispersion in the monomer organic phase with a tendency

towards the interface indicating that the hydrophilicity changed into amphiphilicity. As a result of functionalization, the hydrophiliciy of the modified TiO_2 changes after reaction with the bifunctional molecule (Figure 2.9 b-d). As observed from these Figures, only a very small amount of TiO_2 remained in the water phase, indicating a high degree of functionalization.

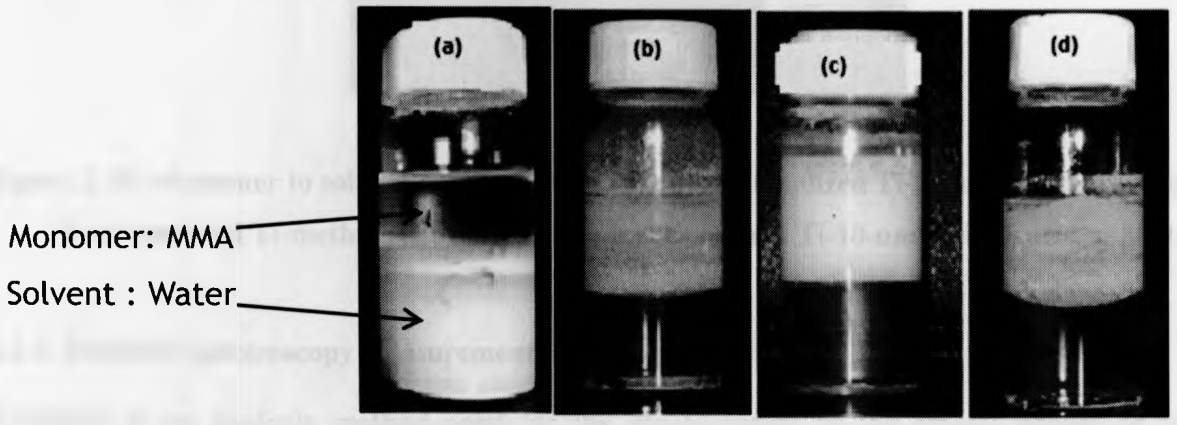

Figure 2.9: Monomer to solvent partitioning of (a) nonfunctionalized calcined TiO_2, (b) Ti-methacrylic acid, (c) functionalized Ti-10-undecenoic acid, (d) functionalized Ti-2-carboxyethyl acrylate at room temperature.

After heating to 80 °C, the functionalized TiO_2 has a higher tendency toward the interface of the water and monomer layers. Figure 2.10 shows the dispersion of functionalized TiO_2 in monomer to solvent partitioning at 80 °C. Both (a) and (b) show a better dispersion in the monomer phase compared to (c). Dispersion of titanium dioxide functionalized with 10-undecenoic acid in monomer becomes more unstable on increasing the temperature, compared to the methacrylic acid and 2-carboxyethyl acrylate. This unexpected result is attributed to weak chemical bond formation between titanium dioxide and 10-undecenoic acid, as the structure of 10-undecenoic acid has a longer chain length which should provide better steric stabilization.

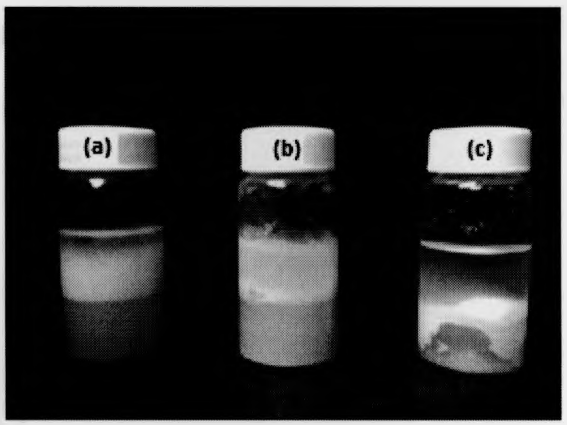

Figure 2.10: Monomer to solvent partitioning with (a) functionalized Ti-2-carboxyethyl acrylate, (b) functionalized Ti-methacrylic acid and (c) functionalized Ti-10-undecenoic acid at 80 °C.

2.3.4. RAMAN spectroscopy measurements

RAMAN is an analysis method used for the identification of the crystal phases of titanium dioxide with the peaks showing crystallinity of titanium. As shown in Figure 2.11, the strong peak in the RAMAN spectrum at 150 cm^{-1} belongs to the anatase phase of n-TiO_2. The split peaks observed at 450 and 608 cm^{-1} are exclusive to anatase and rutile TiO_2 respectively (Zhang et al. 2000). These sharp peaks reduce in the case of functionalized TiO_2 compared to the non-functionalized TiO_2, which may be due to either a reduction of the crystallinity of the surface of TiO_2 after functionalization, or an enhanced surface coverage. The peaks suggest the presence of TiO_2, except for in the case 10-undecenoic acid where very small peaks can be observed. RAMAN scattering as a local probe is very sensitive to crystallinity and microstructures of materials. The functionalizing agents used for functionalization have amorphous structure. The reduction observed in the intensity for the functionalized TiO_2 compared to nonfunctionalized TiO_2 is attributed to the presence of bifunctional monomers on the surface of titanium (Gbureck et al. 2000).

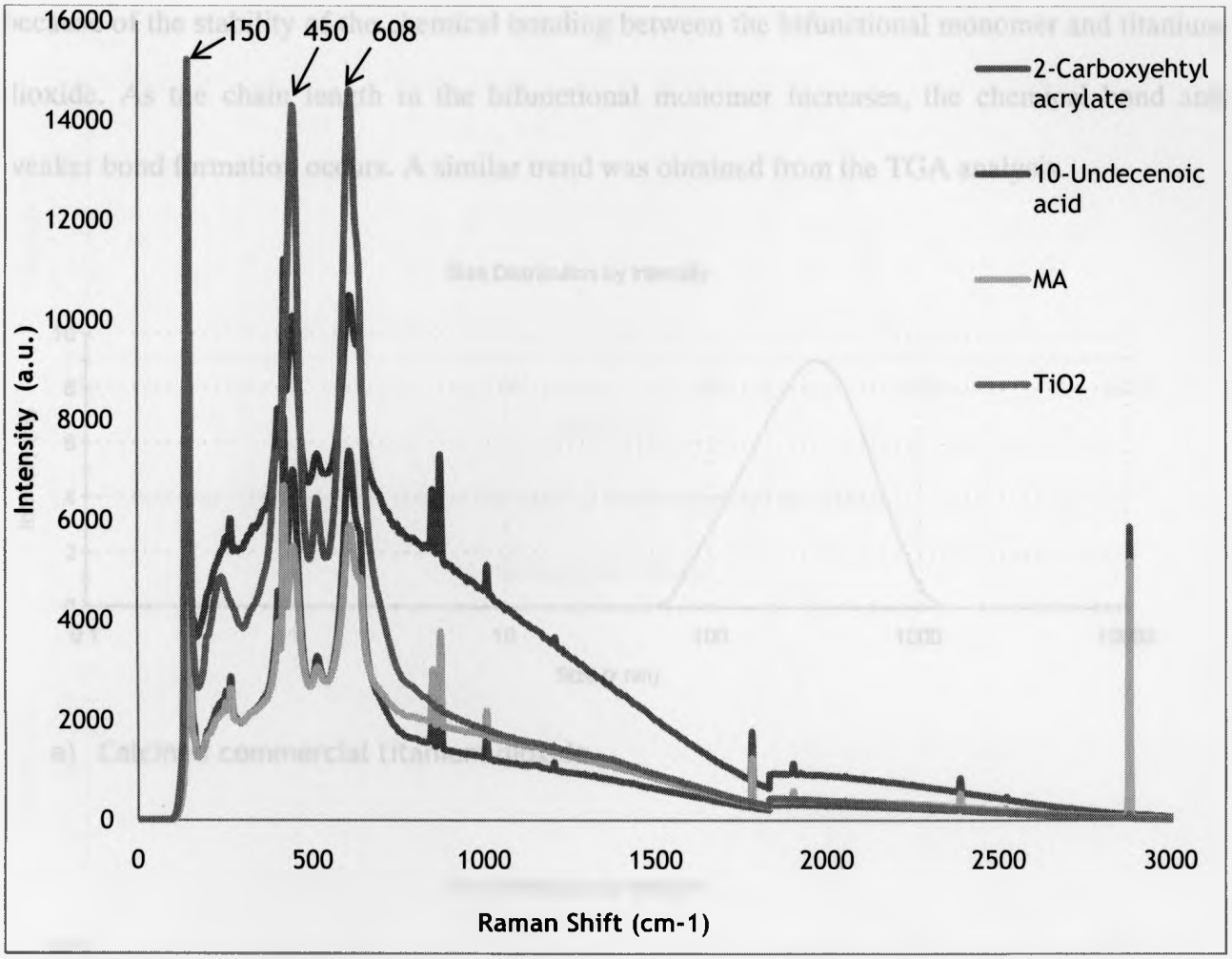

Figure 2.11: Raman graph of n-Ti functionalized by 2-caboxyethyl acrylate, methacrylic acid, 10-undecenoic acid and nonfunctionalized n-TiO_2.

2.3.5. Dynamic Light Scattering (DLS)

Figure 2.12 shows the dynamic light scattering of the nonfunctionalized and functionalized titanium dioxide (0.5wt % in deionised water) providing the particle size distribution (PSD) of the commercially used n-TiO_2 as shown in Figure 2.12a. The size distribution of commercial TiO_2 is in the range of 100-1000 nm, with average size of 200 nm. The highest increase in intensity is observed when TiO_2 is functionalized with methacrylic acid. The intensity percentage decreases as the chain length of the bifunctional molecules increases. This could be

because of the stability of the chemical bonding between the bifunctional monomer and titanium dioxide. As the chain length in the bifunctional monomer increases, the chemical bond and weaker bond formation occurs. A similar trend was obtained from the TGA analysis.

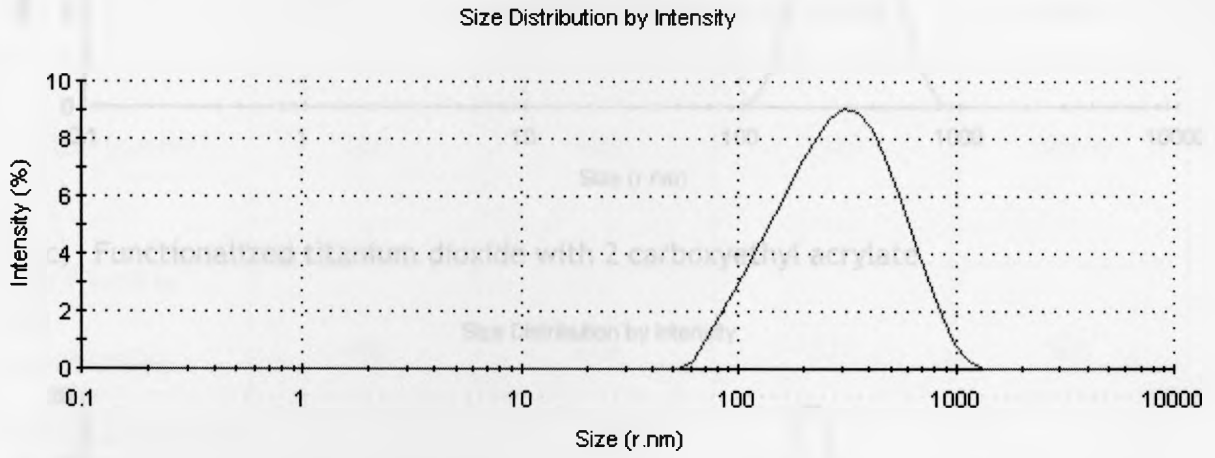

a) Calcined commercial titanium dioxide

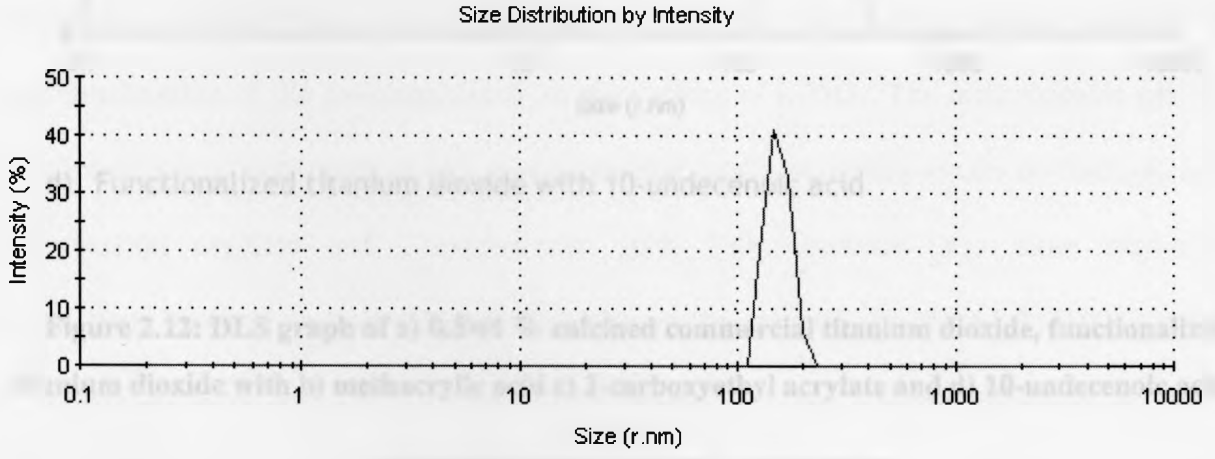

b) Functionalized titanium dioxide with methacrylic acid

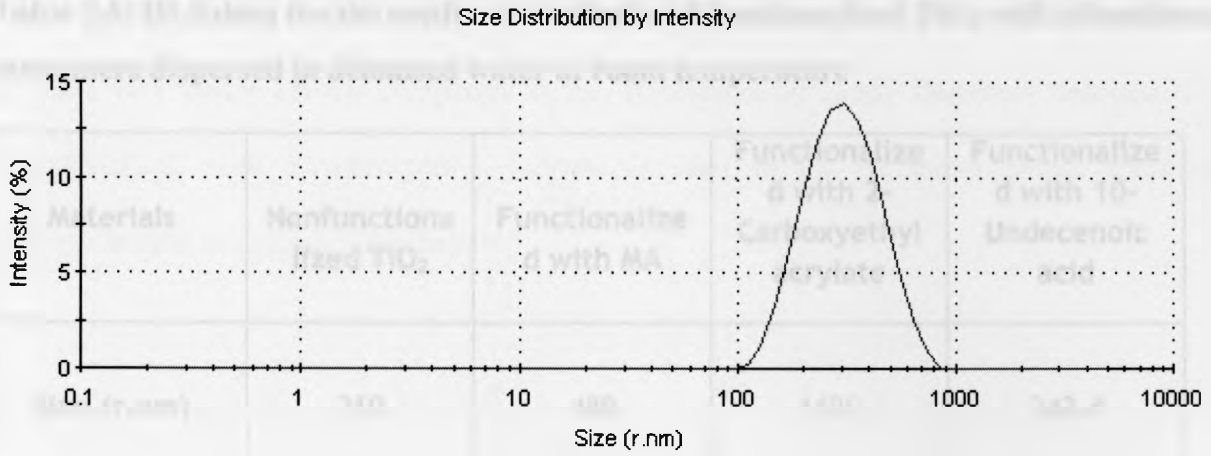

c) Functionalized titanium dioxide with 2 carboxyethyl acrylate

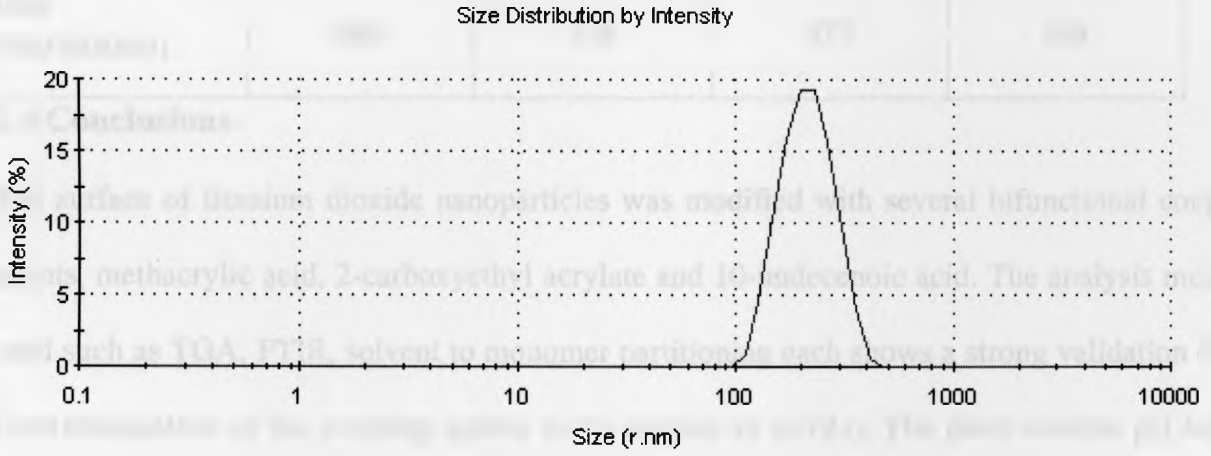

d) Functionalized titanium dioxide with 10-undecenoic acid

Figure 2.12: DLS graph of a) 0.5wt % calcined commercial titanium dioxide, functionalized titanium dioxide with b) methacrylic acid c) 2-carboxyethyl acrylate and d) 10-undecenoic acid in deionised water at room temperature.

Table 2.5: DLS data for the nonfunctionalized and functionalized TiO_2 with bifunctional monomers dispersed in deionised water at room temperature

Materials	Nonfunctionalized TiO_2	Functionalized with MA	Functionalized with 2-Carboxyethyl acrylate	Functionalized with 10-Undecenoic acid
Size (r.nm)	210	480	1129	342.4
PDS(Particle size distribution)	480	748	577	501

2.4 Conclusions

The surface of titanium dioxide nanoparticles was modified with several bifunctional coupling agents, methacrylic acid, 2-carboxyethyl acrylate and 10-undecenoic acid. The analysis methods used such as TGA, FTIR, solvent to monomer partitioning each shows a strong validation of the functionalization of the coupling agents to the surface of n-TiO_2. The most suitable pH for the functionalization is observed to be 5.5 in examining functionalization agents methacrylic acid, 2-carboxyethyl acrylate and 10-undecenoic acid. TiO_2 modified was more organophilic. Interactions between methacrylic functionalities on the polymer chains and the TiO_2 surface are extremely effective, and a strong nano-crystal stabilization and uniform dispersion in the matrix were obtained. The functionalizing agents investigated were found suitable to be used for functionalizing the surface of titania, MA (methacrylic acid) was discussed in the work done by khaled et. al.(Khaled 2009)being a very good choice for functionalizing surface of TiO_2. 2-carboxyethyl acrylate and 10-undecenoid acid both show good potential for the purpose of functionalization as well.

Based on the results obtained by the different analysis tests, it was decided that 2-carboxyethyl acrylate is a better choice compared to the 10-undecenoic acid. Therefore titanium dioxide functionalized with 2-carboxyethyl acrylate is used in the monomer phase microfluidics polymerization is explained in chapter 3.

CHAPTER 3: POLYMERIZATION OF METHYL METHACRYLATE REINFORCED WITH n-TiO_2

3.1 Introduction

Drug delivery technology presents an interesting interdisciplinary challenge for the pharmaceutical, chemical engineering, biomaterials and medical industries. Polymeric microspheres have recently attracted significant attention, and many researchers have studied their use in a wide variety of medical and biological applications. Various polymers have been used as implant carriers for local delivery of antibiotics for the treatment of bone infections. PMMA has been used extensively as a prosthetic material in dental and mandibular corrections and as a bone cement in hip joint reconstruction. Implanted methyl methacrylate polymers appear to be well tolerated if the implants are monomer-free and under a certain threshold size. PMMA and its copolymeric microspheres with incorporated antibiotics are frequently used in the treatment of fractures and ostemies (i.e.surgical opening made in the skin as a way for waste products to leave the body) (Sivakumar, Rao 2000).

Polymer nanocomposites offer dramatically enhanced mechanical and physical properties, including stiffness and heat resistance, gas and solvent barrier properties, flame retardance, and enhanced optical transparency. In addition, these improvements in nanocomposite properties are achieved at very low loadings of the nanoscale inorganic component (<5wt%) while traditional microcomposites usually require a much higher loading of filler i.e. 25-40 wt%. In addition, for the past decade there has been a tremendous interest in synthesizing hollow polymeric microspheres for a variety of applications including encapsulants for the controlled release of drugs and enzymes, fillers, pigments, catalysts, and adsorption materials for sound(Liu et al. 2008).

Polymeric microspherical particles have a wide range of applications with biological and analytical applications including column supports for chromatography, beads for flow cytometry and in the recovery of DNA and proteins. Other applications are photonics, diagnostics and tissue engineering. The properties of each individual particle are critical to their technological function. With this in mind, monodispersity, chemistry, porosity, shape and size are very important. Production of polymeric microspheres can be carried out by conventional polymerization methods, including bulk, solution, emulsion, and suspension polymerization. In this chapter polymerization of MMA (methyl methacrylate) using traditional precipitation polymerization and a novel microfluidics method based on interfacial polymerization are compared. Interfacial polymerization describes polymerization of two reactants carried out at the interface between oil and water liquid phases, each containing one of the reactants, where temperature employed is usually in the range 0-50 ^{o}C (Odian 2004). The polymerization rate is usually diffusion-controlled, since the rates of diffusion of reactants to the interface are slower than the rate of reaction of the two functional groups. There is always a supply of both reactants at the interface due to diffusion from the organic and aqueous phases.

As the aqueous phase contains a stabilizer, a general rule is that the polymer stabilizer should be soluble in the dispersant, cover most of the particle surface, and provide a repulsive interaction between particles that is longer-ranged than the attractive van der waals forces. Addition of surfactants in microencapsulation procedures is important for the formation of the emulsion. The main requirement of any surfactant is not to have impurities which would interfere with the polymerization. The microfluidics approach will be examined with the modeling of the flow described using Fluent and gambit software as a single phase flow and the T-junction experimental set up in chapter 4.

3.2. Materials and Methods

Commercial Titanium (IV) oxide, nanopowder mixture, < 100 nm (BET) 99.5 % trace metal basis (Sigma-Aldrich), initiator AIBN (2,2′-Azobis(2-methylpropionitrile) (Toronto Research Company), crosslinker 1,4-butanediol dimethacrylate (95% Sigma-Aldrich), THF (tetrahydrofuran), (PVA) (99+% hydrolyzed, Sigma-Aldrich) and MMA monomer (99.99wt%, Sigma-Aldrich) were purchased from Sigma-Aldrich. MMA monomer (99%, Sigma-Aldrich, inhibited with 10-100ppm monomethyl ether hydroquinone) was passed through an inhibitor removal column (capacity 3L at 100 ppm hydroquinone, Sigma-Aldrich) before use.

Precipitation polymerization approach: The experimental procedure for polymerization of methyl methacrylate reinforced with n-TiO_2 powders (2wt%) included dispersion of the nano titania functionalized by the coupling agent (Methacrylic Acid, 2-carboxyethylacrylate, 10-undecenoic Acid) in a solution of methyl methacrylate (MMA)(4 wt%), in the presence of initiator AIBN (2,2′-Azobis(2-methylpropionitrile)(0.1wt%), 1,4-Butanediol dimethacrylate (2wt%) and THF (tetrahydrofuran) with the aid of ultrasonic agitation for 30 minutes. The mixture was added to a three neck round bottom flasks containing 100 ml THF solvent followed by heating the reaction content to 65 ^{o}C for 24 hours with constant stirring under argon gas. The reactor was heated by a heating mantle (Glas-Col 1662868) controlled by a voltage regulator (Powerstat 3PN116C) as shown in chapter 2. The reaction product was separated by centrifugation and then dried under vacuum at 100 ^{o}C over night.

Microfluidics approach: Two infusion syringe pumps from KD Scientific, pump 1 (Legato 2200) was used for pumping the oil phase consisting of MMA (methylmethacrylate) monomer and AIBN (2,2-azobisisobutyronitrile) initiator and titanium dioxide functionalized by the functionalizing agents. Pump 2 (Legato 1100) was used for pumping the aqueous phase, PVA

(poly vinyl alcohol) (1 wt %) aqueous in water. A PEEK Micro TEE of 0.006 thru hole, stainless steel Micro-TEE inner diameter of 1/16" (1500 μm) Teflon and peek tubing with inner diameter of 100, 250, 500 microns and outer diameter of 1/16"(1500 μm) were purchased from Upchurch Scientific.

A microfluidic device was built using a Micro-TEE (P-890, Upchurch) to prepare monodisperse or narrow-disperse emulsions and PMMA spheres with and without n-TiO_2 particles. The Micro TEE was placed vertically, as shown in Figure 3.1. The oil phase flow containing MMA (methyl methacrylate) and AIBN initiator was pumped into the side arm of the Micro-TEE using an infusion multiple syringe pump (KD scientific pump, Inc.), while the aqueous phase flow (1.0 wt. % PVA in water) was introduced to the top arm of the Micro-TEE by an infusion pump (KD scientific pump, Inc.) with each inlet equipped with a check valve to minimize the chance of back flow to the system. The formed emulsion was then directed into a 10 mL reservoir solution containing 1.0 wt. % PVA to facilitate the interfacial polymerization, placed directly underneath the Micro-TEE at room temperature. The connections between the Micro-TEE and the pumps and the reservoir solution were made using Teflon® FEP and PEEK tubings. The experiments carried out to obtain the microspheres were conducted at room temperature. The ratio of the oil phase and water phase was varied (1:5, 1:10, 1:15, and 1:20 ratios) to confirm the best flowrate to obtain the most uniform size microspheres.

The emulsion was collected for 5 minutes and then the vial was capped and placed on steel rollers and rotated at a rate of 30 rpm for 24 hours at 70 °C. The resulting microcapsules were washed twice with deionized water in the centrifuge tube to remove unreacted PVA. The emulsion formed was then placed under the light microscope (Zeiss) apparatus with the images captured. To reinforce the PMMA with inorganic, TiO_2 functionalized with 2-carboxyethyl

acrylate as explained in the previous chapter was introduced in the monomer phase and the polymerization was carried out in the Micro-TEE apparatus. The oil phase contained 0.03 gm of functionalized TiO_2 with 2-carboxyethyl acrylate, 0.025 gm of AIBN, 10 ml of MMA. The water phase contains (1wt %) PVA in water with PVA acting as a surfactant stabilizer for the polymerization process. Figure 3.1 shows a schematic diagram of the microfluidics experimental setup used in the current research.

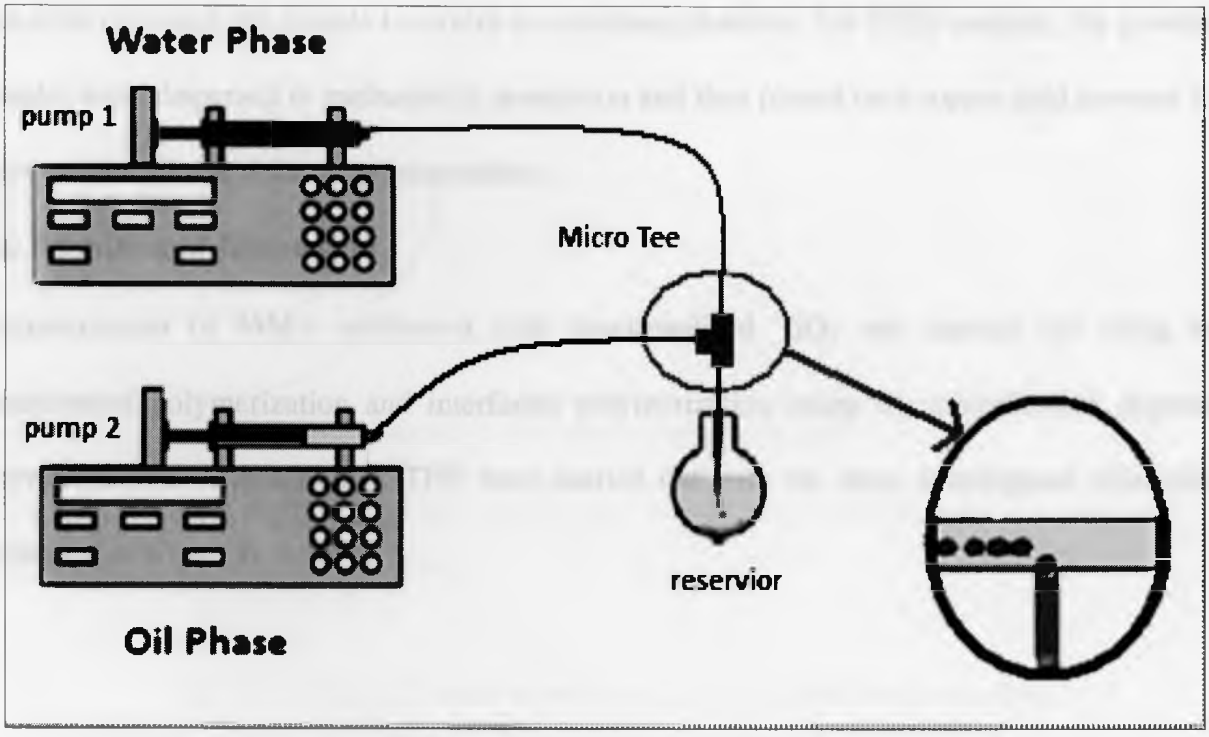

Figure 3.1: Schematic diagram of microfluidics system.

Characterization: Thermogravimentric analysis (TGA) was performed using a Mettler-Toledo TGA/SDTA851^e from 25 to 1000 ^oC at a heating rate of 20 ^oC/min under nitrogen atmosphere. RAMAN analysis was performed using a Kaiser optical system (RXN1-785) with 5 times exposure and 20 times accumulation.

Light microscope (ZEISS) with the DIC and BF method was used to capture images of droplets at room temperature. Fourier transformer infrared (FTIR) was performed using a Thermo

Scientific* Smart iTR with Diamond ATR Crystal at room temperature. Dynamic light scattering (DLS) was performed using Zetasizer Nano series, Nano S model ZEN 1600 particle size analyser at room temperature. PMMA solution was prepared in 50% glycerol and water. The morphologies of the samples were examined using Scanning Electron Microscopy (SEM) (Model LEO 1530) and Transmission Electron Microscopy (TEM) (Model JEOL 2010F). Samples for SEM imaging were prepared by applying the powder directly to a carbon adhesive tape after exposing the sample to oxuim in a vacuum chamber. For TEM analysis, the powdered samples were dispersed in methanol by sonication and then placed on a copper grid covered with holey carbon film and dried by evaporation.

3.4. Results and Discussion

Polymerization of MMA reinforced with functionalized TiO_2 was carried out using both precipitation polymerization and interfacial polymerization using the microfluidics approach. Polymerizations with MMA in THF were carried out with the three investigated bifunctional molecules as shown in Scheme 2.

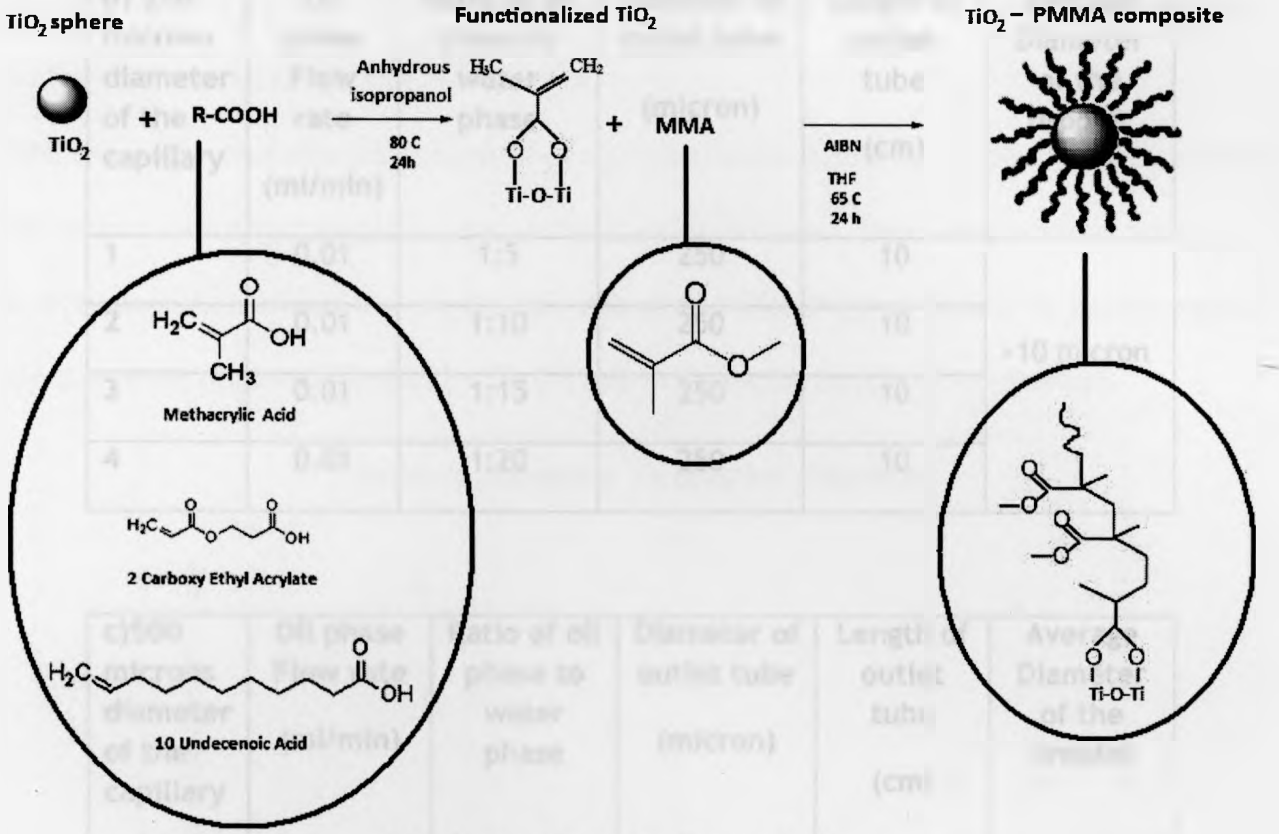

Scheme 2: Polymerization mechanism

Table 3.1 shows the experimental conditions under which the polymerizations of MMA in microfluidics system were carried out.

Table 3.1: Experimental conditions for the microfluidics system.

a) 100 microns diameter of the capillary	Oil phase Flow rate (ml/min)	Ratio of oil phase to water phase	Diameter of outlet tube (micron)	Length of outlet tube (cm)	Average Diameter of the droplet
1	0.01	1:5	100	10	10 micron
2	0.01	1:10	100	10	
3	0.01	1:15	100	10	
4	0.01	1:20	100	10	

b) 250 microns diameter of the capillary	Oil phase Flow rate (ml/min)	Ratio of oil phase to water phase	Diameter of outlet tube (micron)	Length of outlet tube (cm)	Average Diameter of the droplet
1	0.01	1:5	250	10	>10 micron
2	0.01	1:10	250	10	
3	0.01	1:15	250	10	
4	0.01	1:20	250	10	

c)500 microns diameter of the capillary	Oil phase Flow rate (ml/min)	Ratio of oil phase to water phase	Diameter of outlet tube (micron)	Length of outlet tube (cm)	Average Diameter of the droplet
1	0.01	1:5	500	10	Close to 1 micron
2	0.01	1:10	500	10	
3	0.01	1:15	500	10	
4	0.01	1:20	500	10	

Experiments were conducted at room temperature and under atmospheric pressure. The effect of flowrate and the diameter of the outlet capillary were studied. Four ratios of the flowrates (1:5, 1:10, 1:15, and 1:20) for three capillary diameters; 100, 250, 500 microns were studied as shown in Table 3.1. As shown in Figure 3.2, the results show that increasing the diameter of the capillary (outlet tube) decreases the size of the droplets obtained. It was observed that increasing the ratios of the flowrates of the oil phase and the water phase affects the size of the droplets as

well. The most suitable ratio observed is 1:10. This is consistent for the three investigated capillary diameters i.e.100, 250, 500 microns.

If the to-be-dispersed phase is composed of a polymerizable liquid, the droplets can be hardened downstream either by thermal or photo-induced polymerization. Depending on how complete is the polymerization within the droplet, the size of the final polymer particle is usually smaller than that of the originated droplet by 2–10% due to the higher density of the polymer.

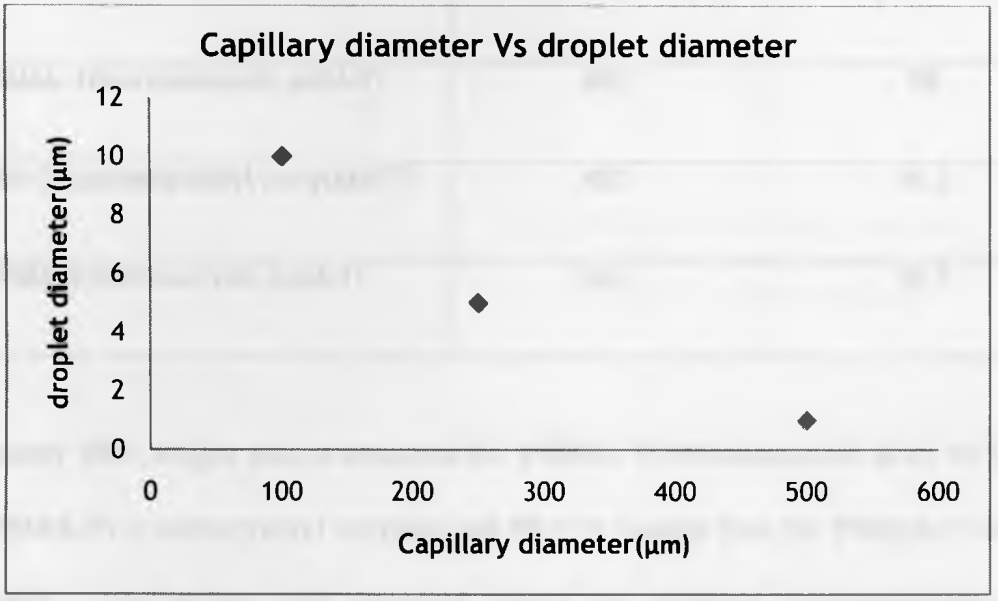

Figure 3.2: Graph of change of droplet size with respect to capillary diameter.

To avoid clogging by hydrolysis and polymerization of the MMA inside the Micro-TEE, the system was flushed with solvent immediately after use.

3.4.1. TGA

As was explained in chapter 2, the thermogravimetric analysis shows the weight loss of the material due to temperature treatment. Figures 3.3 and 3.4 show the TGA graphs of precipitation polymerization of MMA in THF and the microfluidics polymerization of MMA in the Micro-TEE, respectively. Figure 3.3 shows the weight loss for the polymerized MMA reinforced with

TiO_2 functionalized with: a) 10-undecenoic acid, b) 2-carboxyethylacrylate and c) methacrylic acid. The weight loss with respect to temperature observed in the TGA graph for each polymerization experiment is shown in Table 3.2.

Table 3.2: TGA result for the PMMA-Ti functionalized with the bifunctional monomers.

Materials	Temperature (°C)	Weight loss (%)
PMMA-10-uncedecoic acid-Ti	400	98
PMMA-2-carboxyethyl acrylate-Ti	400	98.5
PMMA-methacrylic acid-Ti	400	98.1

Approximately 98% weight loss is observed for PMMA-Ti-10-undecenoic acid, 98.5 % weight loss for PMMA-Ti-2-carboxyethyl acrylate and 98.1 % weight loss for PMMA-Ti-methacrylic acid at 400°C. The weight loss observed shows the polymer functionalization agent is decomposed leaving the TiO_2 component. In all three cases there is close to 2 wt% not burnt in the sample which is agreement with the amount of inorganic n-TiO_2 used as filler in the composite.

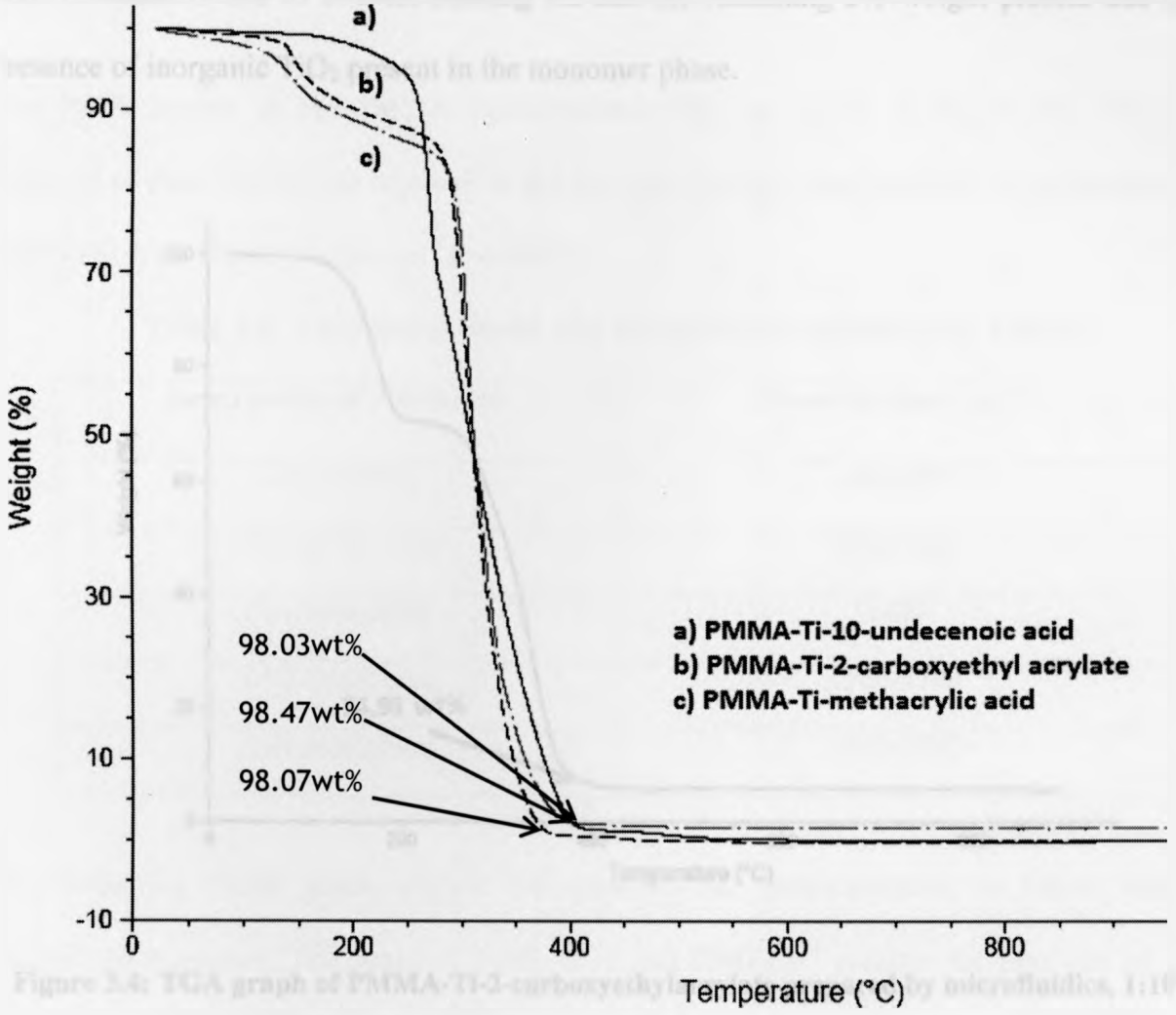

Figure 3.3: TGA graph of PMMA-Ti with titanium functionalized with a) 10-undecenoic acid b) 2-carboxyethylacrylate c) methacrylic acid prepared in THF at 65 °C, 24 hours.

Figure 3.4 shows the TGA graph of the polymerized MMA reinforced by functionalized TiO_2 with 2-carboxyethyl acrylate (0.1 mg) at room temperature using similar experimental conditions for polymerization of MMA in the microfluidics setup having 1:10 for aqeous phase to oil phase ratio. The polymerzation took place in the Micro-TEE and the polymer obtained is the result of interfacial polymerization using the microfluidics approach. The weight loss observed at 0-200 °C is due to the moisture content and unreacted MMA. There is a weight loss close to 95 % at

400 °C which is due to PMMA burning off and the remaining 5% weight present due to the presence of inorganic TiO_2 present in the monomer phase.

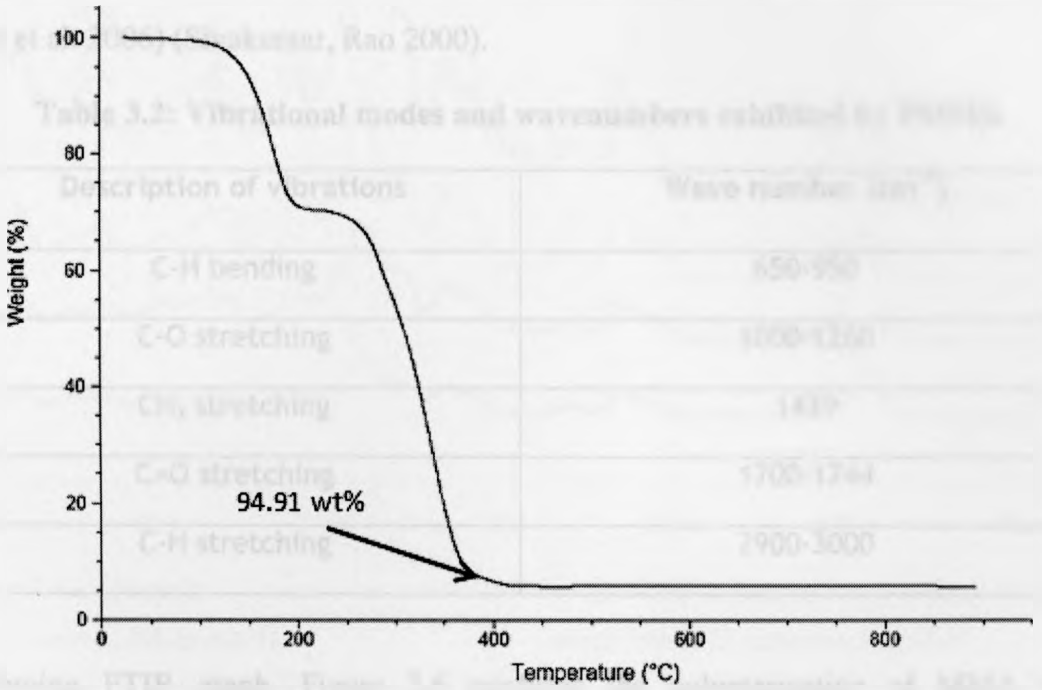

Figure 3.4: TGA graph of PMMA-Ti-2-carboxyethylacrylate prepared by microfluidics, 1:10 oil phase to aqeoues phase ratio at room temperature.

3.4.2. FTIR

The FTIR spectra of the PMMA-functionalized TiO_2 are shown in Figure 3.5. The peaks assigned to pure PMMA are reported in the literature and are listed in Table 3.2 [(Ramesh et al. 2007)(Du et al. 2006) (Sivakumar, Rao 2000).

Table 3.2: Vibrational modes and wavenumbers exhibited by PMMA

Description of vibrations	Wave number (cm^{-1})
C-H bending	650-950
C-O stretching	1000-1260
CH_3 stretching	1439
C=O stretching	1700-1744
C-H stretching	2900-3000

The following FTIR graph, Figure 3.6 confirms the polymerization of MMA with the microfluidics system. The peaks at 1200, 1720 and 2940 cm^{-1} confirm the presence of OCH_3 stretching, C=O carboxylic bond and C-H stretching respectively (Khaled et al. 2007). The absence of any absorbtion peak at 1637 cm^{-1} shows there is no unreacted MMA monomer (Khaled 2009)as the C=C bond of the MMA monomer is converted to a C-C bond in the PMMA polymer (Hojjati 2010).

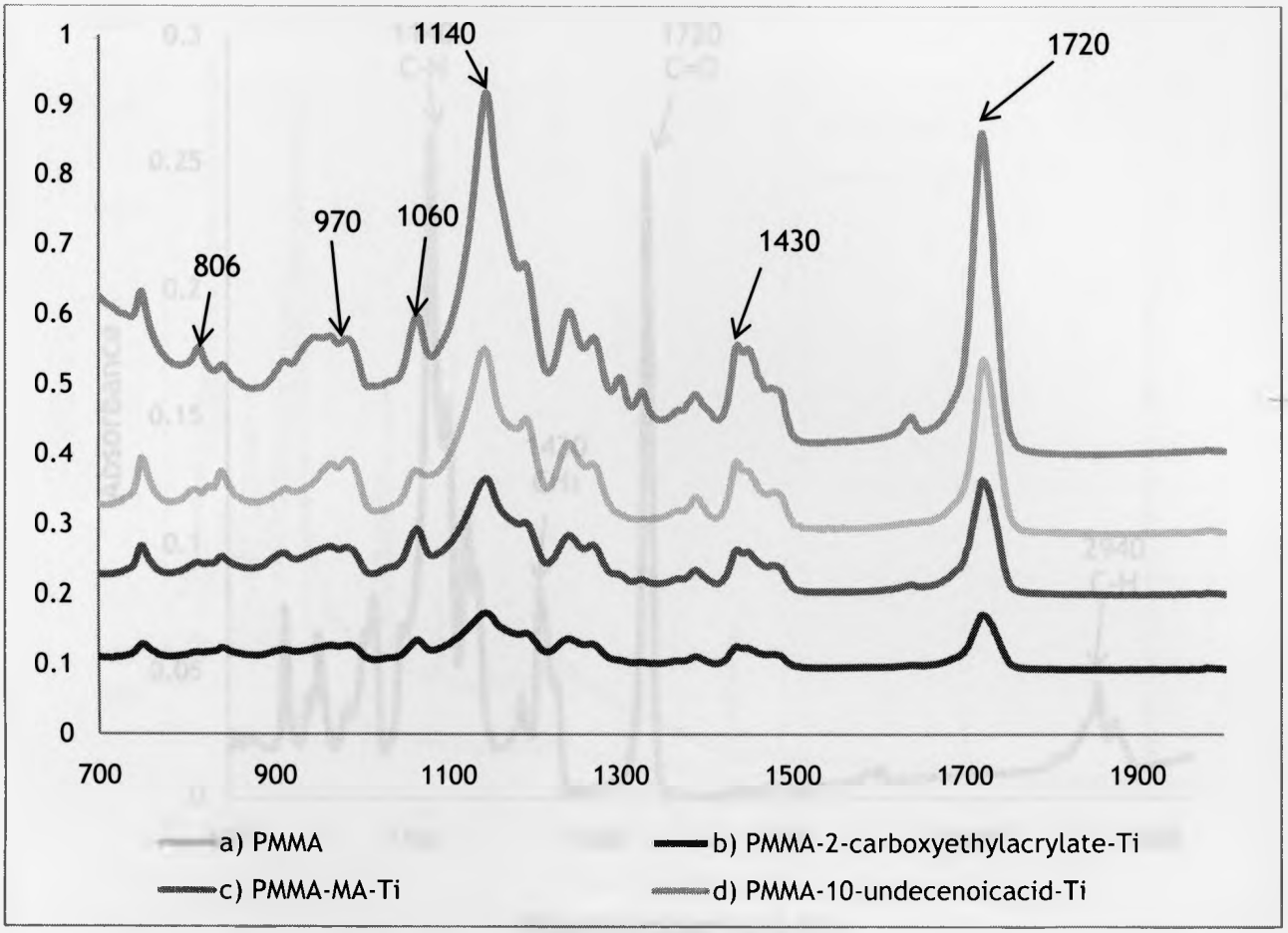

Figure 3.5: FTIR graph of PMMA-Ti-(functionalizing agents) with (conventional) precipitation polymerization.

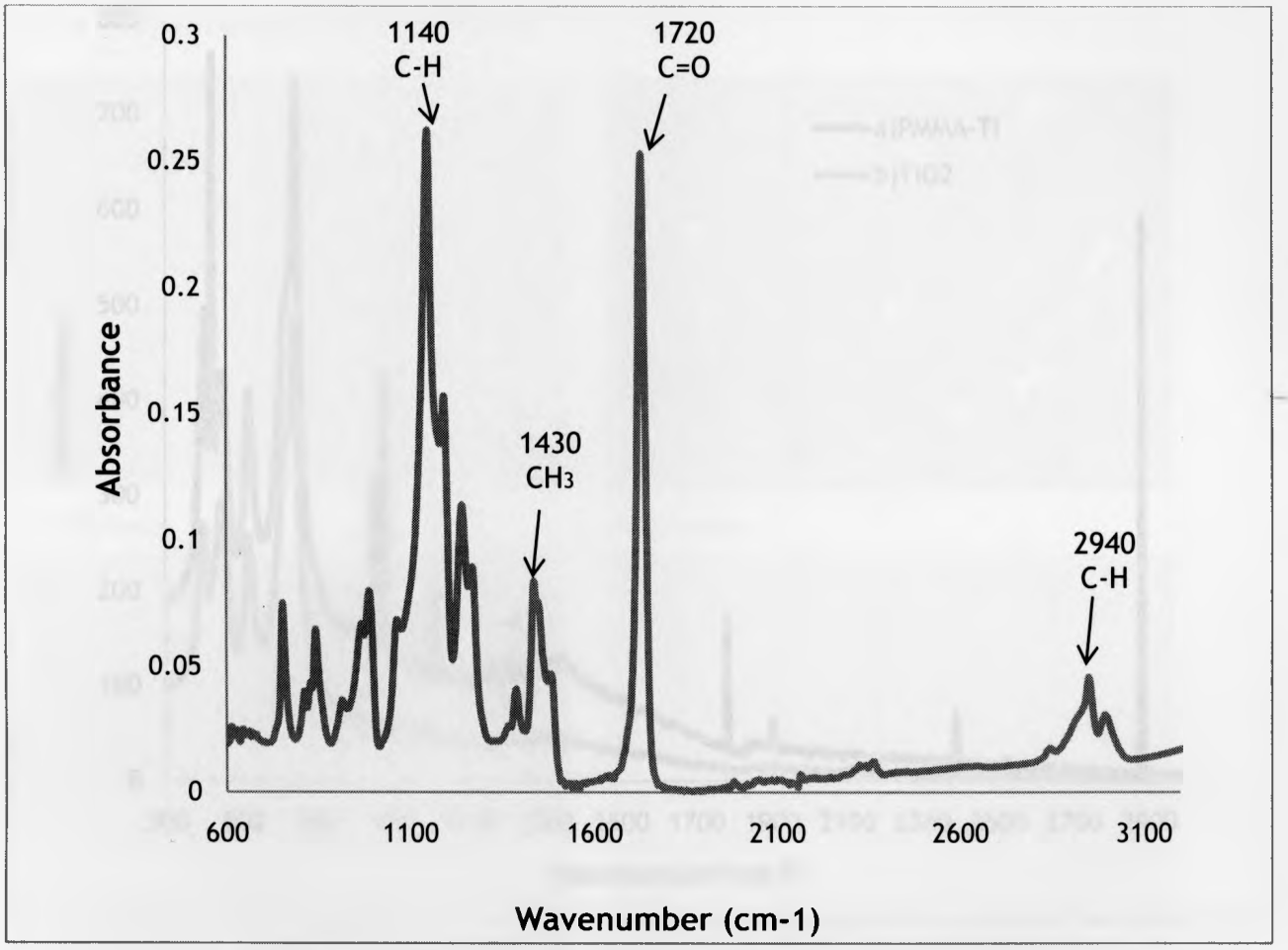

Figure 3.6: FTIR graph of PMMA-Ti by microfluidics system.

3.4.3. RAMAN spectroscopy measurement

As was explained in chapter 2, the RAMAN spectrum can show the crystallinity of TiO_2. Figure 3.7 shows the RAMAN spectrum of the PMMA-Ti nanocomposite obtained by the microfluidics system. The two consecutive peaks close to 500 cm^{-1} are exclusive peaks for the TiO_2. The spectrum of PMMA-Ti shows several peaks, peak 1770 cm^{-1} represents C=O bond in the polymer matrix. Thus PMMA has been grafted from the surface of titanium dioxide. Peaks observed in the range of 500-2000 cm^{-1} are in the finger print region for organic molecules.

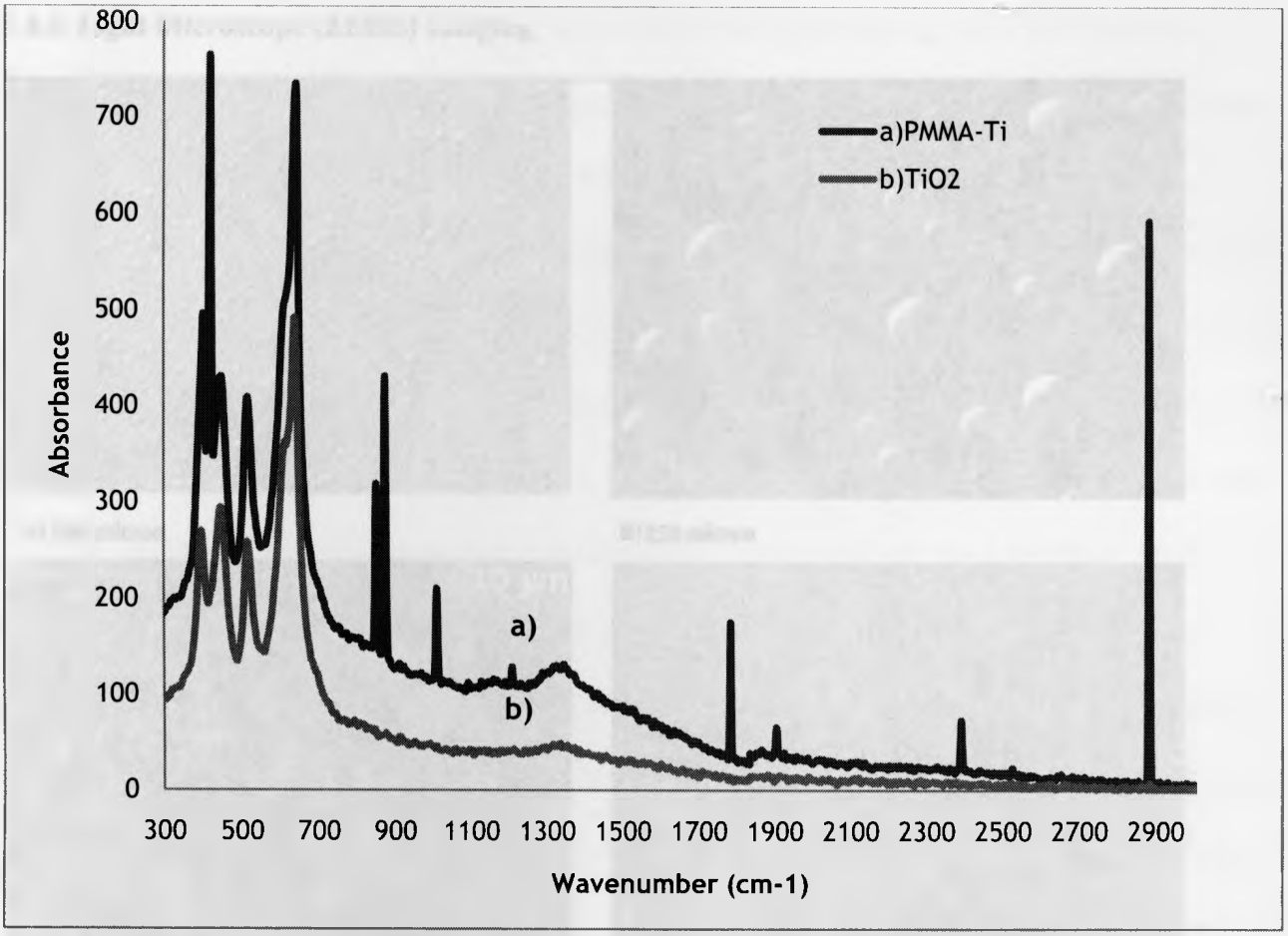

Figure 3.7: RAMAN spectrum of PMMA-Ti microfluidics system.

3.4.4. Light Microscope (ZEISS) Imaging

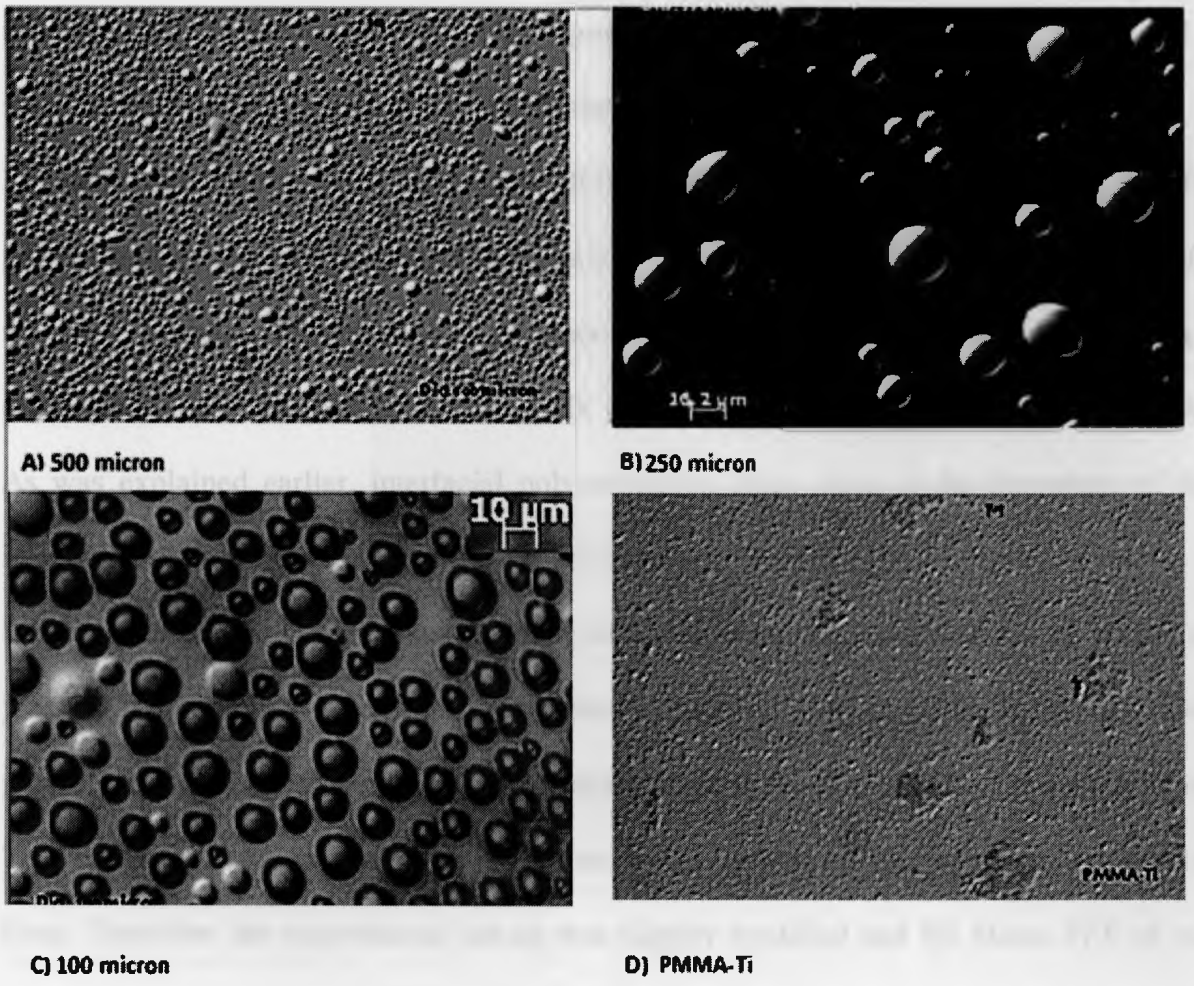

Figure 3.8: Light microscopic images of the microspheres prepared by the microfluidics system having diameter of: A) 500 B) 250, C) 100 micron for outlet, and D) PMMA-Ti spheres.

The spheres obtained with the outlet of 500 microns are smaller than the desired size (i.e. 10-20 microns); this could be the result of a lower residence time. Once the titanium dioxide nanoparticles are introduced in the monomer phase, the droplets formed are smaller in size. The main disadvantage of introducing the n-TiO_2 particles in the Micro-TEE is the possibility of the blockage of the system requiring replacing the Micro-TEE and tubing. As a result of blockage the system can leak causing a pressure drop in the Micro-TEE capillary.

The droplet size increases on decreasing the diameter of outlet tubing, from 500 microns to 250 microns and 100 microns as shown in Figure 3.8. Poly vinyl alcohol (PVA) was used as the stabilizer in the aqueous phase to maintain the structure of the microspheres.

Polymerization taking place in the microfluidics system can potentially be the result of bulk polymerization and not interfacial polymerization if the droplets break up before entering the reservoir solution. Hence, if the polymerization is not carried out at the interface; the microspheres are obtained by solution/bulk polymerization and not interfacial polymerization. As was explained earlier, interfacial polymerization takes place at the interphase of the two immiscible liquids between the oil and water phases.

It was observed that when the outlet tubing of 500 microns was used with a 1/16" (1500 μm) T-junction of stainless steel, the microspheres formed were not the result of interfacial polymerization. Therefore poor mixing is taking place in the Micro-TEE as shown in Figure 3.9. This could be due to a lower residence time in the system for the polymeric microspheres to form. Therefore the experimental set-up was slightly modified and the Micro-TEE of stainless steel was replaced with PEEK Micro-TEE to obtain the desired size and shape for the microspheres. When the vials were placed on the steel roller at 70 ^{o}C, the clear solution started to turn milky white indicating that polymerization was taking place, as the heat from the steel rollers helps facilitate polymerization of the formed microspheres. Furthermore, when the outlet tubing of 500 microns was replaced by 250 microns, the sample collected in the vial showed evidence of interfacial polymerization. Samples were placed on the steel roller having the same temperature as the pervious experiments where no milky white color solution was observed, indicating no bulk or solution polymerization was taking place.

Increasing the flowrate of the continuous phase from 2-6 µl/min was found to reduce the size of the droplets. The high flow rate of the continuous phase (>6µl/min) induces a transition regime from stable droplets to unstable or elongation droplets (Achilleos, Vamvakaki 2010).

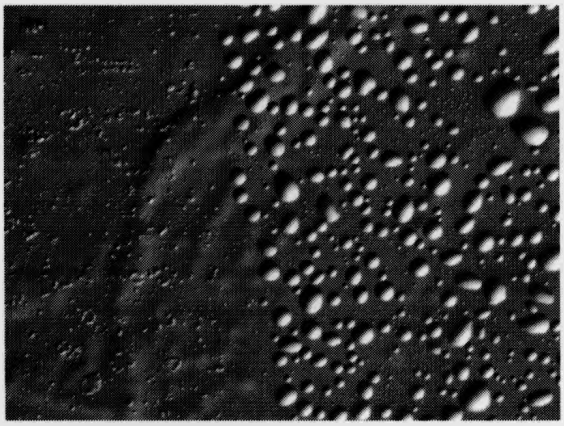

Figure 3.9: PMMA-Ti obtained by microspheres system.

3.4.6. DLS

Dynamic Light Scattering (DLS) is a method to measure the particle size of the products. Basically DLS measures a particle Brownian motion and relates it to its size. Brownian motion is the random movement of particles due to the bombardment by the solvent molecules that surround them. Therefore larger size particles experience slower Brownian motion. DLS data for the PMMA and PMMA-Ti is shown in Figure 3.10. The size distribution of the particles is around 2500 nm (i.e. 2.5 microns). The result obtained from the light microscope (Zeiss) shows the precise size of the microspheres which is close to 10 microns. The particle size for the PMMA produced using the microfluidics is 2.6 Mm and 284 nm for PMMA reinforced with functionalized TiO_2 Figure 3.10 a) and b). The particle size reduces on reinforcing the PMMA with inorganic nanofillers.

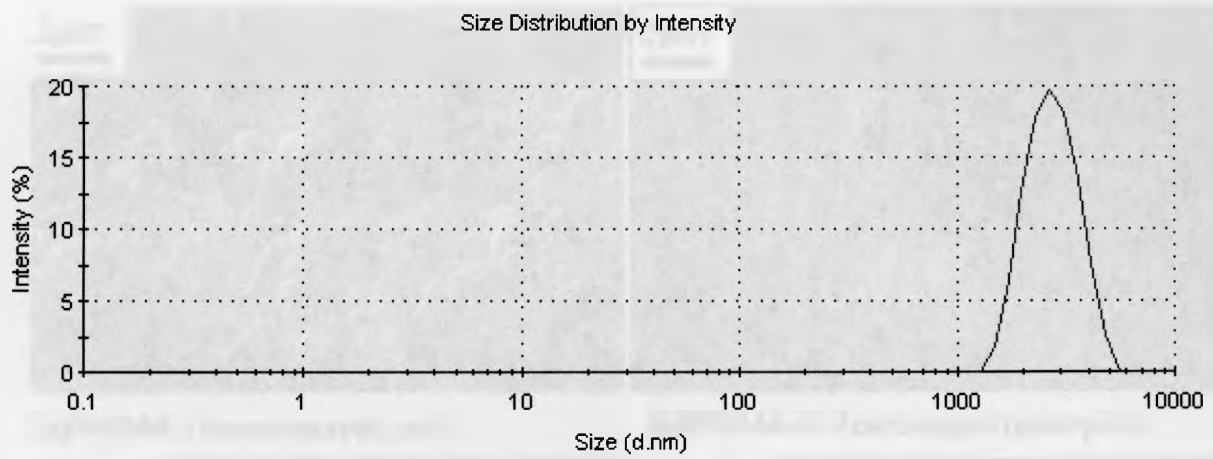

a) PMMA

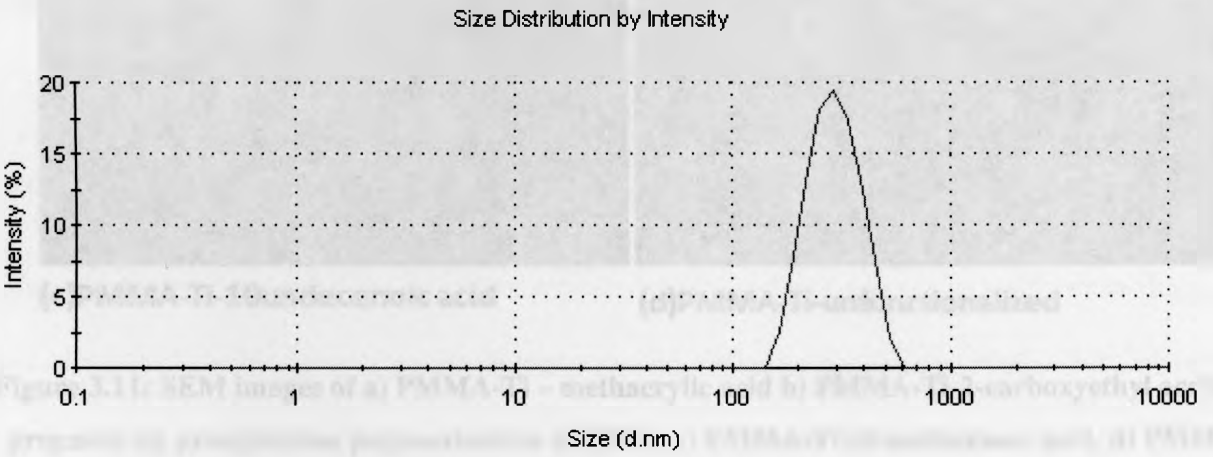

b) PMMA-Ti-2-Carboxyethyl acrylate

Figure 3.10: DLS graph of a) PMMA b) PMMA-Ti (functionalized with Ti-2-Carboxyethyl acrylate) obtained by microfluidics approach.

3.4.5. SEM and TEM

Figure 3.11 shows the SEM images of the PMMA-Ti functionalized with the functionalizing agents and the PMMA-Ti without any functionalization. As can be observed from these images the best uniform morphology is obtained in image a) PMMA-Ti-MA, when precipitation polymerization approach is employed.

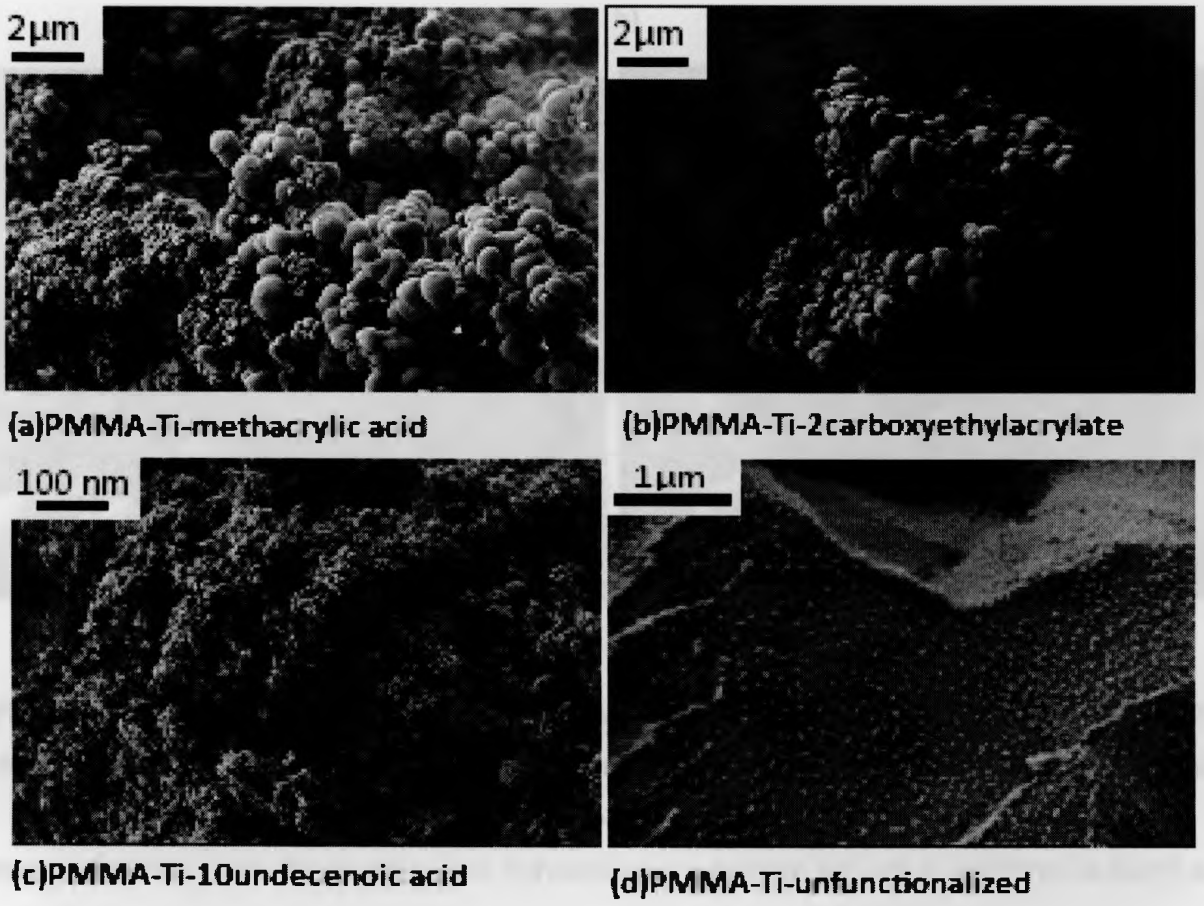

Figure 3.11: SEM images of a) PMMA-Ti – methacrylic acid b) PMMA-Ti-2-carboxyethyl acrylate prepared by precipitation polymerization in THF, c) PMMA-Ti-10-undecenoic acid, d) PMMA-Ti-unfunctionalized.

Figure 3.12 shows the SEM images of the PMMA-Ti-2-carboxyethyl acrylate obtained by the microfluidics procedure using the Micro-TEE using different capillary diameters.

a) b)

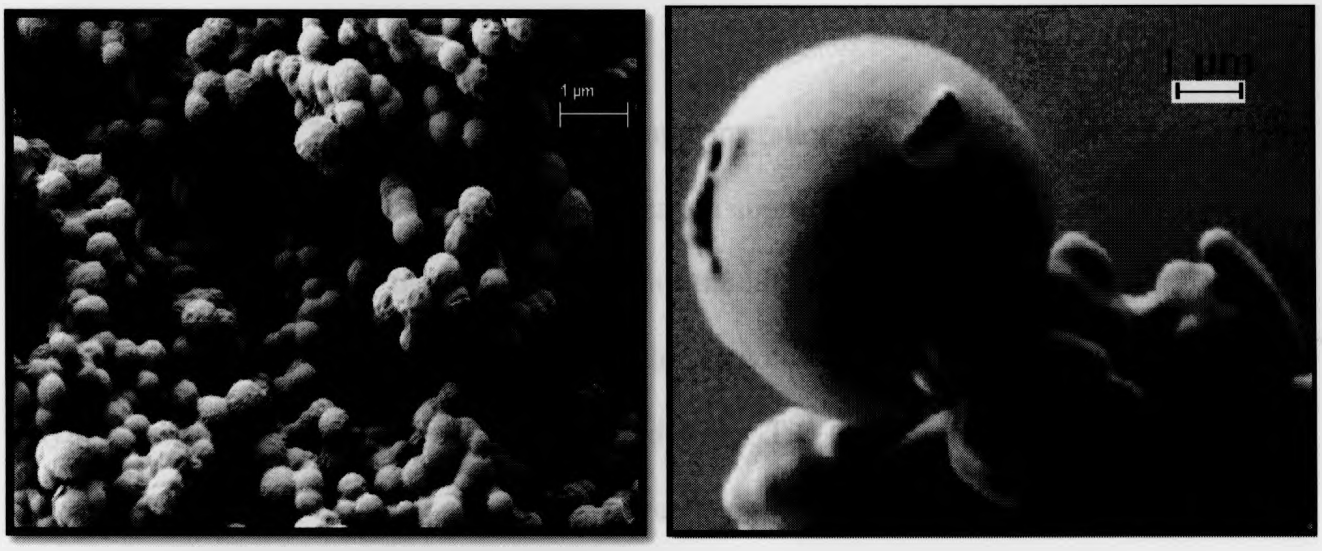

Figure 3.12: SEM image of PMMA-Ti-2-Carboxyethyl acrylate made in Micro-TEE with a) 250 microns diameter of outlet b) 100 microns diameter outlet tube at room temperature with 1:10 oil phase to aqueous phase ratio.

Spheres obtained from the precipitation polymerization method are not as uniform in shape and size compared to the spheres obtained using the microfluidic procedure. Figure 3.12 shows the SEM images of spheres prepared in the Micro-TEE with outlet diameter of the tubing a) 250 microns and b) 100 microns with a length of 10 cm for the outlet. The spheres obtained from precipitation polymerization are smaller, mostly in the nano size range compared to the spheres obtained by the microfluidics procedure which fall in the micron region. However, these results should be viewed with caution as PMMA is electron beam sensitive, resulting in a change of shape and size when subjected to the electron beam within the SEM (Rastogi et al. 2010). This could be the reason for the difference observed in the size of the spheres obtained from the SEM and the light microsphere (Ziess) images.

TEM

TEM images (Figure 3.13) show that there is agglomeration of nano titanium particles in the PMMA matrix when the precipitation polymerization approach is followed. As can be observed the functionalization of the titanium dioxide with the bifunctional monomers methacrylic acid and 2-carboxyethyl acrylate cannot prevent the agglomeration of the nanoparticles in the polymer matrix. The same trend was observed when TiO_2 was functionalized with the 10-undecenoic acid. This agglomeration is not desirable in the polymer matrix which may be due to the high temperatures used during polymerization

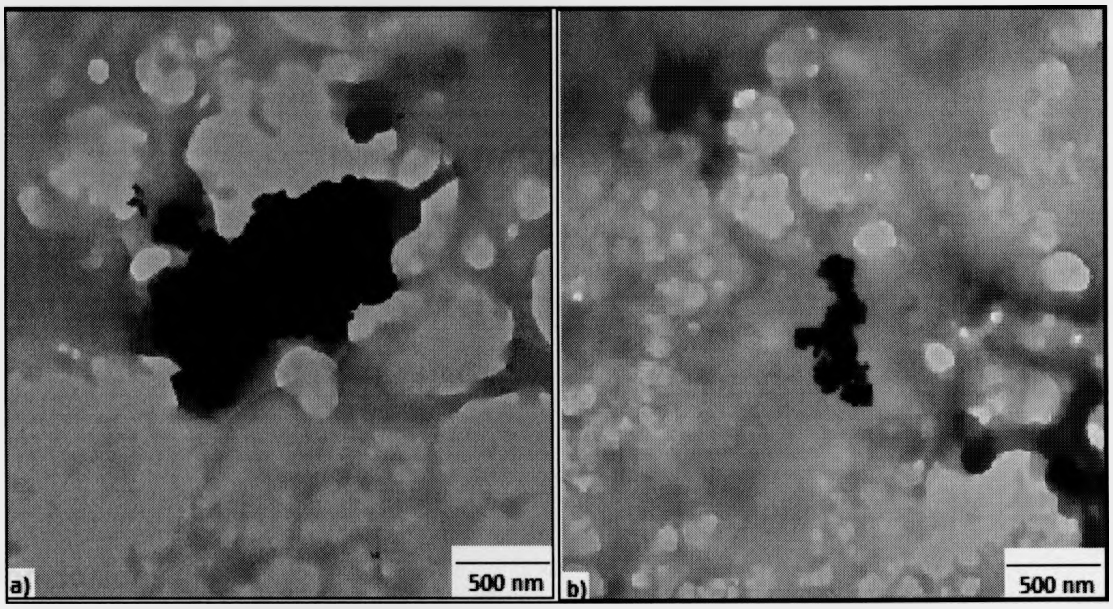

Figure 3.13: TEM image of the PMMA-Ti- a) functionalized by MA b) functionalized by 2-carboxyethyl acrylate, obtained by precipitation polymerization approach in THF at 65 °C.

3.4.7. GPC

Figure 3.14 shows the peak obtained from the PMMA polymer made in the Micro-TEE reactor. The results obtained from the GPC instrument shows the Mw ≈ 350 KDa and PDI (polydispersity index) ≈ 4 for the PMMA obtained by the microfluidics procedure.

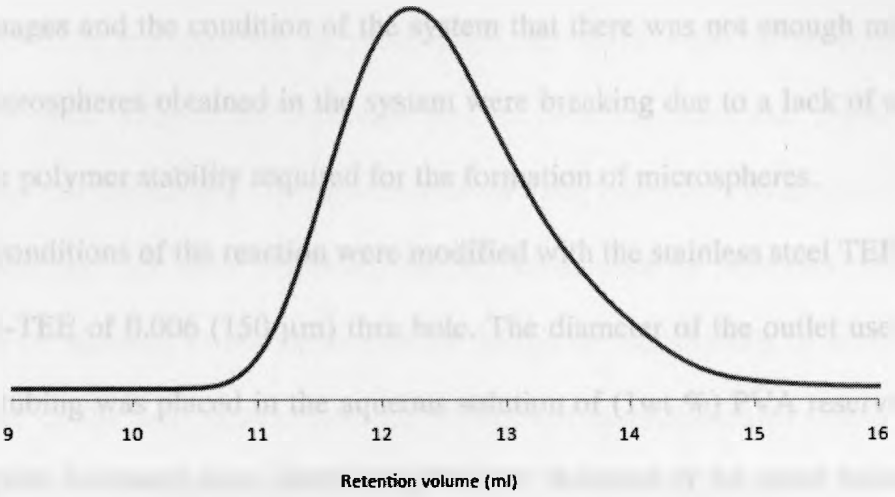

Figure 3.14: GPC graph of PMMA obtained by the microfluidics system.

The molecular weights obtained by GPC fall in the range of average molecular weight for PMMA polymer (M_w 350,000).

Table 3.4: GPC result for PMMA

M_w (molecular weight)	349,824
M_n (molecular number)	86,833
PDI (polydispersity Index)	4

3.5. Conclusions

It was observed that while using the stainless T-junction of 1/16" (1500 μm) inner diameter with no grooving or tempering inside, the microspheres obtained were smaller compared to the peek Micro TEE of 0.006 (150 μm) thru hole . Hence, the stainless steel T gave a poor, mixing of water and oil phase resulting in poor microsphere formation.

The outlet tubing to collect the microspheres was set above the aqueous medium for an initial set of experiments and the results obtained were not satisfactory, but once the outlet was set below

the level of solution in the reservoir, better results were obtained. It was then observed from the microscopic images and the condition of the system that there was not enough mixing in the T-junction, or microspheres obtained in the system were breaking due to a lack of sufficient PVA to help with the polymer stability required for the formation of microspheres.

Therefore the conditions of the reaction were modified with the stainless steel TEE replaced with a PEEK Micro-TEE of 0.006 (150 μm) thru hole. The diameter of the outlet used was reduced and the outlet tubing was placed in the aqueous solution of (1wt %) PVA reservoir. Hence, the size of the droplets increased upon decreasing the inner diameter of the outlet tubing and a better particle size distribution was obtained.

It can also be concluded that the best results were obtained when the 10 micron inner diameter outlet tubing with a 1/10 ratio of oil to aqueous phase at room temperature was employed for the formation of droplets by the microfluidics system. The high temperature of the steel roller helps in decomposition of the initiator (AIBN) resulting in polymerization of MMA and producing polymers with high molecular weight, the constant rotation of steel roller results in uniform temperature distribution for polymerization.

CHAPTER 4: CONCLUSIONS AND RECOMMENDATIONS

In order to use TiO_2 particles for polymerization, its surface has to be modified. Surface modification of nano TiO_2 is an important part of both academic and applied research. A common strategy for the surface functionalization of TiO_2 (and other oxides) is based on using anchoring groups that can carry additional functionalities such as monomer. Reactive organic groups have to be attached to the surface of the inorganic nanocrystals to achieve the desired application. One of the well known methods for surface modification of titania is coating the titanium dioxide with an organic polymer layer. Before surface modification of TiO_2 the surface of TiO_2 was found to be hydrophilic. It contains several OH groups, and has no chemical affinity with organic monomer. Thus the adsorption of MMA onto the surface of TiO_2 particles and also surface polymerization are difficult to take place. It was observed that after functionalization of the titanium dioxide surface with the investigated biphasic molecules, polymerization proceeded, and polymer was formed on the surface of the TiO_2 powder.

On the surface of the modified TiO_2 nanopowders, the spreading degree of organic solvents rises, but the spreading degree of water descends based on the water/MMA partitioning studies. This indicates that the wettability of the polymer surface –modified TiO_2 nanopowders in organic solution was improved.

Polymers obtained using the microfluidics system was found to show better size and shape compared to the polymers obtained by traditional polymerization processes.

4.1. Recommendations and future work

Although the formation of polymer microspheres using the experimental microfluidics system increased, there are significant challenges and issues that still need to be addressed. The methods used either lack control over the dimension of the droplets as a result of post modifications of the

beads, or lose the advantages of an on-chip polymerization process. Partial failure such as clogging of the tubing was one of the most important challenges that have to be addressed. This was found to result in leakage or a pressure drop in the system.

As a part of the future work, a series of microfluidic systems can be set up in such a way as to have more than one reaction taking place in the system. The effect of the concentration of the initiator and monomer can be examined by having series of T-junctions, each having different concentrations of monomer and initiator being pumped through their inlets. The data obtained can then be used in determining most suitable reaction conditions for microsphere morphology.

The challenge that has to be addressed is the blockage of the Micro-TEE and tubing due to the presence of the inorganic particles such as TiO_2 in this research. Although the particle size of the titanium dioxide used is less than 100 nm, agglomeration of the nanoparticles while travelling through the microfluidics system led to blocking of the system. As the flowrate of the oil phase is very slow, i.e. in the rate of microliters per minute, the n-TiO_2 particles dispersed in the oil phase can settle down in the tubing or through the Micro-TEE reactor. It was observed that not all the n-TiO_2 powders were functionalized, therefore some settled in the system and caused the blocking of the tubing and the Micro-TEE, although the whole setup was washed with solvent immediately after use. Hence the tubing had to be replaced and the experiments were repeated. As the diameter of the outlet tubing decreases, the problem of blockage rises.

4.2. Limitations

Agglomeration and sedimentation of nanoparticles may occur during the flow of the nanoparticles dispersed in the monomer phase through micro-channels at very small flow velocities which can affect the droplet formation process.

The challenge in controlling the flow in the system arises while using the 0.006" (150 μm) thru-holes Micro-TEE compared to using the stainless steel 1/16" (1500 μm) TEE. This can be explained based on the geometry, as the radius of the TEE decreases, the size of the droplets increases. This is due to an increase in the surface tension forces, but at the same time this can result in clogging of the system which was found to be a problem. Nevertheless, the microfluidics approach has significant potential to replace the traditional batch reactor polymerization for producing microspheres.

The main challenge of the type of microfluidic system used in this research is the sedimentation of the nano titanium dioxide, although the n-TiO_2 was dispersed in the monomer phase before injection into the Micro-TEE, there was sedimentation of particles observed in the system. As a result, some sort of mixing or adding additional stabilizers is required to keep the particles from settling in the syringe. Ideally, microfluidics devices should allow for rapid and cost-effective prototyping. Materials that are popular in microfluidics system that are compatible for organic reactions are "liquid Teflon" and those made from silicon/glass. However, these approaches require expensive monomer synthesis or specialized techniques, and the resulting microfluidics devices are easily clogged with polymer debris, causing problems for smaller lab-scale systems.

References

Achilleos, D.S. & Vamvakaki, M. 2010, "End-Grafted Polymer Chains onto Inorganic Nano-Objects
", *Materials 2010, 3(3), 1981-2026; doi:10.3390/ma3031981,* vol. 3, no. 3, pp. 1981-2026.

Anderson, J.D. 1995, "Computational Fluid Dynamics: The Basics With Applications", *Science/Engineering/Math, .*

Baroud, C.N. & Willaime, H. 2004, "Multiphase flows in microfluidics", *Comptes Rendus Physique,* vol. 5, no. 5, pp. 547-555.

BIOMET 2011, , *BIOMET.* Available: http://www.bonecement.com/cementing-techniques/bonecement/history.

Chang-Hyung, C., Jae-Hoon, J., Taek-Sung, H. & Chang-Soo, L. 2009, "In Situ Microfluidic Synthesis of Monodisperse PEG Microspheres", *Macromolecular Research, Vol. 17, No. 3, pp 163-167 (2009),* vol. 17, no. 3, pp. 163-167.

Cohen, I., Hui Li, H., Hougland, J.L., Mrksich, M. & Nagel, S.R. 2001, "Using Selective Withdrawal to Coat Microparticles", vol. 292, no. 5515, pp. 265-267.

Dendukuri, D. & Doyle, P.S. 2009, "The Synthesis and Assembly of Polymeric Microparticles Using Microfluidics", *Advanced Materials,* vol. 21, no. 41, pp. 4071-4086.

Dobson, K.D. & McQuillan, A.J. 2000, "In situ infrared spectroscopic analysis of the adsorption of aromatic carboxylic acids to TiO_2, ZrO_2, Al_2O_3, and Ta_2O_5 from aqueous solutions", *Spectrochimica Acta Part A: Molecular and Biomolecular Spectroscopy,* vol. 56, no. 3, pp. 557-565.

Du, X., Fu, Y., Sun, J., Han, X. & Liu, J. 2006, "Complete UV emission of ZnO nanoparticles in a PMMA matrix", *Semicond. Sci. Technol. 21 (2006) 1202–1206,* vol. 21, pp. 1202-1206.

Gbureck, A., Gbureck, U., Kiefer, W., Posset, U. & Thull, R. 2000, "FT-Raman Spectroscopic Investigations of Titanium Alkoxides with Polymerizable Organic Ligands

", *Volume 54, Issue 3, Pages 88A-113A and 331-459 (March 2000),* vol. 54, no. 3, pp. 88A-113A.

Ginebra, M.P., Albuixech, L., Fernández-Barragán, E., Aparicio, C., Gil, F.J., San Román, J., Vázquez, B. & Planell, J.A. 2002, "Mechanical performance of acrylic bone cements containing different radiopacifying agents", *Biomaterials,* vol. 23, no. 8, pp. 1873-1882.

Graaf, S.v.d., Nisisako, T., Schroën, C.G.P.H., Sman, R.G.M.v.d. & Boom, R.M. 2006, "Lattice Boltzmann Simulations of Droplet Formation in a T-Shaped Microchannel", *Langmuir,* vol. 22, no. 9, pp. 4144-4152.

Hamming, L.M., Qiao, R., Messersmith, P.B. & Catherine Brinson, L. 2009, "Effects of dispersion and interfacial modification on the macroscale properties of TiO_2 polymer–matrix nanocomposites", *Composites Science and Technology,* vol. 69, no. 11-12, pp. 1880-1886.

Hessel, V., Hofmann, C., Lo¨b, P., Lo¨hndorf, J., Lo¨we, H. & Ziogas, A. 2005, "Aqueous Kolbe-Schmitt Synthesis Using Resorcinol in a MicroreactorLaboratory Rig under High-p,T Conditions", *Institut fu¨r Mikrotechnik Mainz GmbH, Carl-Zeiss-Strasse 18-20, 55129 Mainz, Germany,* vol. 9, no. 4, pp. 479-489.

Hirata, Y., Kamikakimoto, J., Nishimoto, A. & Ishihara, Y. 1992, "Interaction between α-alumina surface and polyacrylic acid", *1992, vol. 100, no1, pp. 7-12 (19 ref.),* vol. 100, no. 1, pp. 7-12.

Hojjati, B. 2010, *Synthesis and characterization of TiO_2nanocomposites via reversible addition fragmentation chain-transfer polymerization,* School of Graduate and Postdoctoral Studies, University of Western Ontario, London, Ont.

Huang, J. & Kaner, R.B. 2004, "Nanofiber Formation in the Chemical Polymerization of Aniline: A Mechanistic Study", *Angewandte Chemie International Edition,* vol. 43, no. 43, pp. 5817-5821.

Jones, D.W. & Rizkalla, A.S. 1996, "Characterization of experimental composite biomaterials", *Journal of Biomedical Materials Research,* vol. 33, no. 2, pp. 89-100.

Keng-Shiang, H., Tzung-Heng, L. & Yu-Cheng, L. 2006, "Manipulating the generation of Ca-alginate microspheres using microfluidic channels as a carrier of gold nanoparticles", *Lab on a Chip,* vol. 6, no. 7, pp. 954-957.

Khaled, S.M.Z. 2009, *Development of a new generation of bone cements using nanotechnology,* School of Graduate and Postdoctoral Studies, University of Western Ontario, London, Ont.

Khaled, S.M.Z., Charpentier, P.A. & Rizkalla, A.S. 2010, "Synthesis and characterization of poly(methyl methacrylate)-based experimental bone cements reinforced with TiO_2–SrO nanotubes", *Acta Biomaterialia,* vol. 6, no. 8, pp. 3178-3186.

Khaled, S.M., Sui, R., Charpentier, P.A. & Rizkalla, A.S. 2007, "Synthesis of TiO_2–PMMA Nanocomposite:Using Methacrylic Acid as a Coupling Agent", vol. 23, no. 7, pp. 3988–3995.

Lee, K. & Rhee, S. 2009, "The mechanical properties and bioactivity of poly(methyl methacrylate)/SiO_2–CaO nanocomposite", *Biomaterials,* vol. 30, no. 20, pp. 3444-3449.

Link, D.R., Anna, S.L., Weitz, D.A. & Stone, H.A. 2004, "Geometrically Mediated Breakup of Drops in Microfluidic Devices", vol. 92, no. 5.

Liu, G., Li, L., Yang, X. & Dai, Z. 2008, "Preparation of silica/polymer hybrid microspheres and the corresponding hollow polymer microspheres with functional groups", vol. 19, no. 12, pp. 1922-1930.

Lott, J.R. 2006, "Reversible Addition-Fragmentation Chain-Transfer (RAFT) Polymerization in Grafting Polymer Chains from TiO2 Nanoparticles", *August 2006,* .

Luis, S.V. & GarcÃa-Verdugo, E. 2010, *Chemical reactions and processes under flow conditions,* RSC Publishing, Cambridge, UK.

Murshed, S., Tan, S., Nguyen, N., Wong, T. & Yobas, L. 2009, "Microdroplet formation of water and nanofluids in heat-induced microfluidic T-junction", *Microfluidics and Nanofluidics,* vol. 6, no. 2, pp. 253-259.

Mursheda, S.M.S., Leong, K.C. & Yanga, C. 2008, "Thermophysical and electrokinetic properties of nanofluids – A critical review", *3 December 2007; accepted 9 January 2008. Available online 16 January 2008.,* vol. 28, no. 17-18, pp. 2109-2125.

Nakagawaa, K., Iwamotoa, S., Nakajima, M., Shonob, A. & Satohb, K. 2004, "Microchannel emulsification using gelatin and surfactant-free coacervate microencapsulation", *Journal of Colloid and Interface Science Volume 278, Issue 1, 1 October 2004, Pages 198-205,* vol. 278, no. 1, pp. 198-205.

Nguyen, N. & Wereley, S.T. 2006, *Fundamentals and applications of microfluidics,* 2nd edn, Artech House, Boston.

Nie, Z., Xu, S., Seo, M., Lewis, P.C. & Kumacheva, E. 2005, "Polymer Particles with Various Shapes and Morphologies Produced in Continuous Microfluidic Reactors", *J. Am. Chem. Soc., 2005, 127 (22), pp 8058–8063,* vol. 127, no. 22, pp. 8058-8063.

Nisisako, T., Torii, T. & Higuchi, T. 2004, "Novel microreactors for functional polymer beads", *Chemical Engineering Journal,* vol. 101, no. 1-3, pp. 23-29.

Nisisako, T., Torii, T. & Higuchi, T. 2002, "Droplet formation in a microchannel network", *Lab on a Chip,* vol. 2, no. 1, pp. 24-26.

Odian, G.G. 2004, *Principles of polymerization,* McGraw-Hill, New York.

Parallax medical 2011, , *Parallax medical.* Available: http://www.parallaxmed.com/pages/How.

Pasqui, D., Rossi, A., Di Cintio, F. & Barbucci, R. 2007, "Functionalized Titanium Oxide Surfaces with Phosphated Carboxymethyl Cellulose: Characterization and Bonelike Cell Behavior", vol. 8, no. 12, pp. 3965.

Paunesku, T. 2003, "Biology of TiO_2–oligonucleotide nanocomposites", vol. 2, no. 5, pp. 343-346.

Puska, M.A., Kokkari, A.K., Närhi, T.O. & Vallittu, P.K. 2003, "Mechanical properties of oligomer-modified acrylic bone cement", *Biomaterials,* vol. 24, no. 3, pp. 417-425.

Qiyun, Q., Hongwei, G., Ruixiang, P., Qi, C., Xiaohong, G., Fanqing, L. & Mingtai, W. 2010, "Chemically Binding Carboxylic Acids onto TiO_2 Nanoparticles with Adjustable Coverage by Solvothermal Strategy", *American Chemical Society,* .

Quevedo, E., Steinbacher, J. & McQuade, D.T. 2005, "Interfacial Polymerization within a Simplified Microfluidic Device:Capturing Capsules", *J. Am. Chem. Soc., 2005, 127 (30), pp 10498–10499,* vol. 127, no. 30, pp. 10498-10499.

Ramesh, S., Leen, K.H., Kumutha, K. & Arof, A.K. 2007, "FTIR studies of PVC/PMMA blend based polymer electrolytes", *Spectrochimica Acta Part A: Molecular and Biomolecular Spectroscopy,* vol. 66, no. 4-5, pp. 1237-1242.

Rastogi, A., Paik, M.Y., Tanaka, M. & Ober, C.K. 2010, "Direct Patterning of Intrinsically Electron Beam Sensitive Polymer Brushes", *ACS Nano 2010 4 (2), 771-780,* vol. 4, no. 2, pp. 771-780.

Schwalbe, T., Autze, V., Hohmann, M. & Stirner, W. 2004, "Novel Innovation Systems for a Cellular Approach to Continuous Process Chemistry from Discovery to Market", *Org. Proc. Res. Dev., 2004, 8 (3), pp 440–454,* vol. 8, no. 3, pp. 440-454.

Seo, M., Nie, Z., Xu, S., Mok, M., Lewis, P.C., Graham, R. & Kumacheva, E. 2005, "Continuous Microfluidic Reactors for Polymer Particles", *Langmuir, 2005, 21 (25), pp 11614–11622,* vol. 21, no. 25, pp. 11614-11622.

Serra, C.A. & Chang, Z. 2008, "Microfluidic-Assisted Synthesis of Polymer Particles", vol. 31, no. 8, pp. 1099-1115.

Sivakumar, M. & Rao, K.P. 2000, "Synthesis and characterization of poly(methyl methacrylate) functional microspheres", *Reactive and Functional Polymers,* vol. 46, no. 1, pp. 29-37.

Steinbacher, J.L. & McQuade, D.T. 2006, "Polymer chemistry in flow: New polymers, beads, capsules, and fibers", *Journal of Polymer Science Part A: Polymer Chemistry,* vol. 44, no. 22, pp. 6505-6533.

Sugiura, S., Nakajima, M., Kumazawa, N., Iwamoto, S. & Seki, M. 2002, "Characterization of Spontaneous Transformation-Based Droplet Formation during Microchannel Emulsification", .

Tahir, M.N. 2006, "Facile Synthesis and Characterization of Functionalized, Monocrystalline Rutile TiO_2 Nanorods", vol. 22, no. 12, pp. 5209.

Takeuchi, S., Garstecki, P., Weibel, D.B. & Whitesides, G.M. 2005, "An Axisymmetric Flow-Focusing Microfluidic Device", *Volume 17, Issue 8, pages 1067–1072, April, 2005,* vol. 17, no. 8, pp. 1067-1072.

Utada, A.S., Lorenceau, E., Link, D.R., Kaplan, P.D., Stone, H.A. & Weitz, D.A. 2005, "Monodisperse Double Emulsions Generated from a Microcapillary Device", *Science 22 April 2005: Vol. 308 no. 5721 pp. 537-541,* vol. 308, no. 5721, pp. 537-541.

Wade, L.G.J. 2010, *Organic Chemistry,* 7th edn, Pearson Prentice Hall, United State of America.

Wang, W., Zhao, S. & Pan, T. 2009, "Lab-on-a-print: from a single polymer film to three-dimensional integrated microfluidics", *Lab on a Chip,* vol. 9, no. 8, pp. 1133-1137.

Webb, S. 2009, , *Melodies divert droplets*. Available: http://www.webbofscience.com/2009/08/26/melodies-divert-droplets/.

Whitesides, G.M. 2006, "The origins and the future of microfluidics", vol. 442, no. 7101, pp. 368.

Yang, S., Shim, S.E. & Choe, S. 2005, "Stable poly(methyl methacrylate-co-divinylbenzene) microspheres via precipitation polymerization", *Journal of Polymer Science Part A: Polymer Chemistry,* vol. 43, no. 6, pp. 1309-1311.

Zhang, W.F., He, Y.L., Zhang, M.S., Yin, Z. & Chen, Q. 2000, "Raman scattering study on anatase TiO2 nanocrystals", *Journal of Physics D: Applied Physics,* vol. 33, no. 8, pp. 912-916.

Zheng, B., Tice, J.D. & Ismagilov, R.F. 2004, "Formation of Droplets of Alternating Composition in Microfluidic Channels and Applications to Indexing of Concentrations in Droplet-Based Assays", *Anal. Chem., 2004, 76 (17), pp 4977–4982,* vol. 76, no. 17, pp. 4977-4982.

Appendices

Appendix 1: Dimensionless Number's Calculations

Oil Phase; Reynolds number

The Reynolds number relates the ratio of inertial to viscous forces. Viscosity, the internal friction of a fluid, produces a resistance to shear and a tendency for the fluid to move in parallel layers known as laminar flow; and inertia, the tendency of a body in motion to retain its initial motion, counters laminar flow and can ultimately result in turbulent flow. In this research the Reynolds number is calculated as follows;

Reynolds number $\mathrm{Re} = \frac{\rho u D}{\mu} = \frac{QL}{vA}$

Q: flowrate m^3/s, cm^3/s

A: tube cross-sectional area m^2, cm^2

L: characteristic length m, cm

v : kinematic viscosity

$v = \mu/\rho$

$$= \frac{(0.00599 pois, \frac{dyne.s}{cm^2}, \frac{g}{cm,s})}{0.94 \frac{g}{cm^3}}$$

$V = 6.37 * 10^{-3}\ cm^2/sec$

$A = \pi r^2$

$= \pi (150 \text{ micron}/2)^2$

$= \pi (150 * 10^{-4}/2)^2$

$A = 1.767 * 10^{-4} \text{ cm}^2$

For the oil phase of 0.002 ml/min

$$\text{Re} = \frac{0.002 ml/\min * 1.5 cm}{6.37 * 10^{-3} cm^2/\sec * 1.767 * 10^{-4} cm^2}$$

Re = 44.42

Capillary number

The ratio between viscous and capillary forces is given by the capillary number. Capillary is the rise or depression of a liquid in a small passage, such as a thin tube. Water inside a glass capillary tube will have a concave meniscus that is in equilibrium because of a pressure difference across the interface. Such a pressure difference exists whenever a liquid surface is curved (as in the case of liquid drops or soap bubbles), with the higher pressure found on the inner side of the curve. The capillary number is given by:

$$Ca = \frac{U\mu}{\gamma}$$

U= velocity of flow

μ =viscosity of the fluid

γ = surface tension = 23.5 ±3.0 dyne/cm

U (avg. Velocity) =Q/A

$$= \frac{0.002 cm^3 / \min}{\pi(\frac{150}{2} * 10^{-4})^2 cm^2}$$

$$= 0.189 cm / \sec$$

$$Ca = \frac{0.189 cm / \sec * 0.00599 dyne.s / cm^2}{23.5 dyne / cm}$$

$$= 4.82 * 10^{-5}$$

Peclet number

The Peclet number, Pe, provides an indication of the relative importance of diffusion and convection, diffusion being the random thermal motion of molecules within their surrounding environment and convection the transport as a result of bulk motion of a fluid. The Peclet number is defined as :

$$Pe = \frac{U_a H}{D}$$

U_a: Avg. Velocity

H: characteristic length

D: diffusion coefficient of the particle or molecule of interest

$$Pe = \frac{0.189 cm / \sec * 1.5 cm}{1.61 * 10^{-3} cm^2 / \sec}$$

Pe =176.08

Aqueous Phase; Reynolds number

Kinematic viscosity of water at 20 °C ,

$\nu = 1.004*10^{-6}$ m/sec

$A = \pi r^2$

$= \pi (150 \text{ micron}/2)^2$

$= \pi (150*10^{-4}/2)^2$

$A = 1.767 *10^{-4} \text{ cm}^2$

For the aqueous phase of 0.04 ml/min

$$\text{Re} = \frac{0.04 ml/\min * 0.5 cm}{1.004*10^{-6} *10^{4} cm^2/\sec * 1.767*10^{-4} cm^2}$$

Re = 187.8992

Capillary number

$$Ca = \frac{U\mu}{\gamma}$$

U= velocity of flow

μ =viscosity of the fluid

γ = surface tension = 72.8 dyne/cm

U (avg. Velocity) =Q/A

$$= \frac{0.0456 cm^3 / \min}{\pi(\frac{150}{2} * 10^{-4})^2 cm^2}$$

$$= 4.301 cm / \sec$$

$$Ca = \frac{4.301 cm / \sec * 0.0092 dyne.s / cm^2}{72.8 dyne / cm}$$

$$= 5.4354 * 10^{-4}$$

Peclet number

The Peclet number, Pe, provides an indication of the relative importance of diffusion and convection, diffusion being the random thermal motion of molecules within their surrounding environment and convection the transport as a result of bulk motion of a fluid. The Peclet number is defined as :

$$Pe = \frac{U_a H}{D}$$

U_a: Avg. Velocity

H: characteristic length

D: diffusion coefficient of the particle or molecule of interest

$$Pe = \frac{4.301 cm / \sec * 0.5 cm}{2.4 * 10^{-5} cm^2 / \sec}$$

Pe =89604.16

Appendix 2

Computational Fluid Dynamics (CFD) Modelling of Microfluidics Design

Introduction

Researchers have long relied on the use of round-bottomed flasks as a means for carrying out organic polymerization reactions. Recently, microfluidic devices have emerged as a new technology to facilitate organic transformations which provides several advantages over traditional reaction vessels. Continuous flow devices have been used in other fields of research for some time and the potential for adopting this technology in polymerization provides tremendous potential. Interest in miniaturized chemical and biological systems has grown tremendously. Any microfluidics approach follows a simple sequence of steps;

Pump system → mixer → micro device → analytical system

Continuous micro-flow reactors are defined as miniaturized systems consisting of a channel network with dimensions usually ranging from a few to several hundred micrometers in scale. This network of channels is often embedded in silicon or polymers (Luis, GarcÃa-Verdugo 2010). Distinctive properties of microfluidics can be divided into: i) mixing and ii) thermal management.

i) Mixing

The mixing in classical reactors, such as round-bottom flasks and batch reactors is limited to the flow fields created by the stirring bar or impellers. The turbulence and chaotic mixing is a result of convection induced as the fluid approaches the stirring bar or impeller (Steinbacher, McQuade 2006). The shear forces that cause the convection are significantly dampened away from the stirrer and the majority of the round-bottom flask or reactor experiences little to no mixing. As

the fluids are in constant contact in the microfluidics system, the mixing is mainly dominated by diffusion affecting the very slow flowrate of the flows helping in providing better mixing as the two fluids are parallel. The constant flow of two fluids with a very slow flowrate (i.e. ml/hr) allows for better mixing (Hessel et al. 2005).

ii) Thermal management

In any reaction system a critical variable to control is the heating and cooling. The inability to control either accurately can result in very slow reactions needing heat or potentially leading to explosions as a result of a runaway reaction requiring additional cooling. Reactions with more than one product (either kinetic or thermodynamic) are very sensitive to temperature. Batch reactors often offer more than one pathway due to its broad temperature profile (Schwalbe et al. 2004). A micro-reactor is a safe reactor for highly exothermic polymerizations due to its high degree of control that limits side reactions such as premature chain termination or chain transfer. The main advantage that micro-reactor systems provide is the precise control over the fluid behaviour (Steinbacher, McQuade 2006).

Simulation and modelling in microfluidics is an approach used to compare and confirm obtained experimental results. Computational fluid dynamics (CFD) is the science of predicting fluid flow, heat transfer, mass transfer, chemical reactions, and related phenomena by solving mathematical equations that represent physical laws using a numerical process (Anderson 1995). This branch of fluid mechanics uses numerical methods and algorithms to analyze and solve problems that involve fluid flow. The fluid may be in liquid, gas or loose particle form, or a combination of these. Computers are used to perform the calculations required to simulate the interaction of liquids and gases with surfaces defined by boundary conditions for complex

problems. CFD analysis complements experimentation so as a result reduces the total effort required in the laboratory.

The fundamental basis of almost all CFD problems is the Navier–Stokes equations (equation 4.1), which define any single-phase fluid flow:

$$\rho \frac{\partial u}{\partial t} + \rho(u.\nabla) = -\nabla\rho + \nabla.(\eta[\nabla_{u} + (\nabla_{u})^{T}]) \qquad (4.1)$$

where, u is the velocity vector, ρ is the fluid density, p is the pressure, η is the fluid viscosity (it's assumed constant), and T is the temperature. These equations can be simplified by removing terms describing viscosity to yield the Euler equations. Further simplification by removing terms describing vorticity yields the full potential equations. Finally, these equations can be linearized to yield the linearized potential equations.

A CFD model of the flow of the oil phase and aqueous phase in the T-junction experimental microfluidics reaction is implemented in this chapter. This model represents the inlet and outlet flows and mixing taking place in the micro-TEE reactor. Compared to conventional processes, microfluidic-assisted processes offer the possibility to precisely control not only the size of the particle but also its shape, morphology, and composition(Serra, Chang 2008).

Methods and Procedure

Droplets are formed due to the shear force between the PVA solution (aqueous phase) and monomer solution (oil phase) with these two phases being immiscible. The hydrophilic aqueous phase and the hydrophobic oil phase form a W/O emulsion in the microfluidic channel (Dendukuri, Doyle 2009). The formation of the droplet at a junction is governed by the competition between the viscous stress and the surface tension forces. The mechanism of droplet formation can be explained by the relation of interfacial tension between the two phases and the presence of a drag force. Interfacial tension is the cohesive energy present at the interface and

rises from the imbalance force between the molecules of two different phases (i.e. oil phase and aqueous phase). Interfacial tension leads to an accumulation of free energy at the interface. This excess energy is called the surface free energy i.e. the energy required to increase the surface area of the interface. Large interfacial tension holds the droplet detachment from the intersection of the Micro-TEE. At the same time, the extruded aqueous phase volume grows as the flow proceeds which means that the effective drag force (i.e. opposing force) increases as the droplet grows. When the droplet growth reaches a stage that the drag force is large enough to overcome the interfacial tension force, the droplet will be detached and carried away downstream. Thus, the force balance between the shear force and the interfacial tension force determines the droplet size formed inside the micro-channel. Figure 4.1 gives a schematic drawing of the droplet formation, 4.1 (a) and (b) show that there is no droplet formation when the interfacial tension is more than the drag force, while (c) shows the droplet formation and detachment. A 3D similar to that of the schematic drawing is shown in Figure 4.2 for better visualization of the droplet formation.

As can be observed from equation 4.2, the drag force depends on the velocity of the fluid. Equation 4.3 shows an increase in the flowrate results in an increase in the velocity while keeping the area unchanged (Nguyen, Wereley 2006), i.e.

$$F_D = \frac{1}{2}\rho u^2 C_D A \tag{4.2}$$

$$u = \frac{Q_d \, or \, Q_C}{A} \tag{4.3}$$

where ρ is the fluid density, u is the velocity, C_D is the drag coefficient, Q_d and Q_c are the flowrates of the dispersed phase (oil phase) and the continuous phase (aqueous phase) and A is the reference area. Therefore from equations 4.2 and 4.3 it can be concluded that an increase in

the flowrate of the phases in the system increases the drag force and results in the formation of droplets.

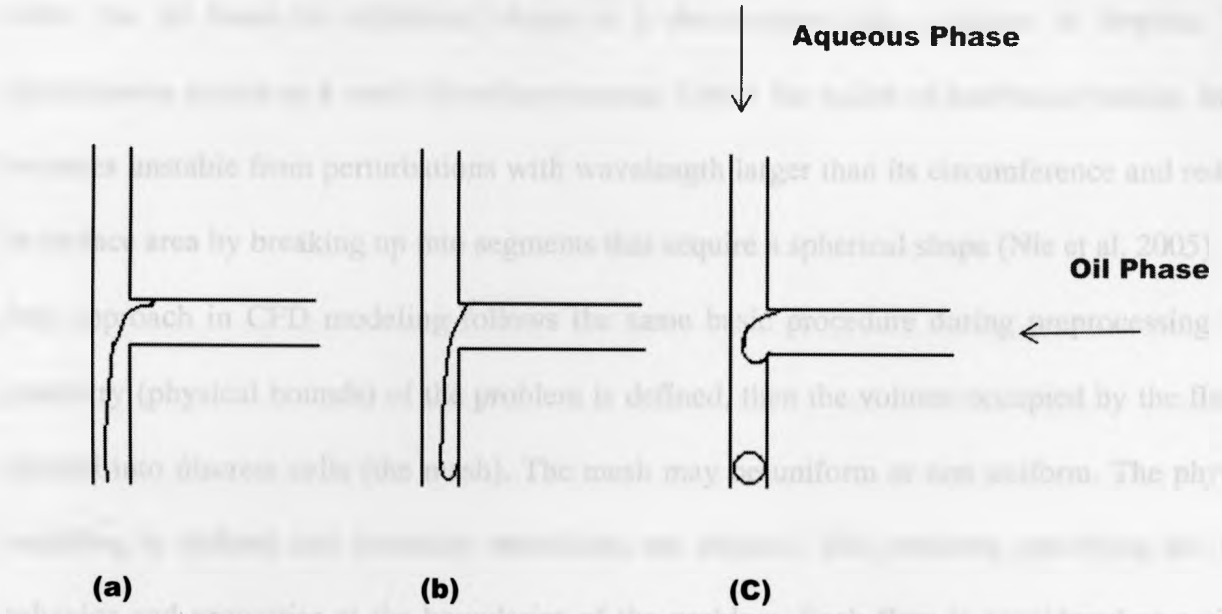

Figure 1: Schematic digram of the droplet formation in the T-junction.

Figure 2: Droplet detachment in the T-junction obtained by the comsol software.

Generation of the droplets from a liquid cylindrical jet occurs due to a Rayleigh-Plateau hydrodynamic instability. As can be seen in Figure 4.2 jet of liquid having a constant radius falls because of gravity, with the liquid length increasing and reaching a critical value. At this critical value, the jet loses its cylindrical shape as it decomposes into a stream of droplets. This phenomenon occurs as a result of surface tension. Under the action of interfacial tension, the jet becomes unstable from perturbations with wavelength larger than its circumference and reduces its surface area by breaking up into segments that acquire a spherical shape (Nie et al. 2005).

Any approach in CFD modeling follows the same basic procedure during preprocessing. The geometry (physical bounds) of the problem is defined, then the volume occupied by the fluid is divided into discrete cells (the mesh). The mesh may be uniform or non uniform. The physical modeling is defined and boundary conditions are defined. This involves specifying the fluid behavior and properties at the boundaries of the problem. Each flow is considered as a single phase flow and the simulation is started and the equations are solved iteratively as a steady-state or transient. Finally a postprocessor is used for the analysis and visualization of the resulting mathematical solution (Anderson 1995).

The mixing of the two fluids in the Micro-TEE reactor shown in Figure 4.3 is modeled with the help of Fluent modeling program. The geometry of the T-junction system was designed in the gambit, and then the geometry was meshed. The model designed uses two dimensional parameters and mixed flow method with steady state conditions and specific boundary conditions in a single phase.

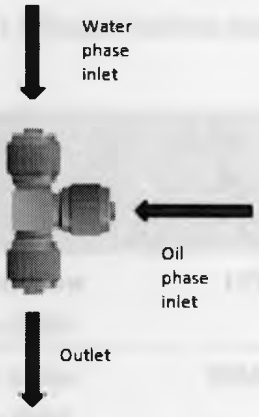

Figure 3: Micro-TEE used in the microfluidics system.

Fluent software was used to run the codes for the flowrate, density and pressure. In this work the mixed flow equation was solved for the flow rates of the oil phase and the aqueous phase. For this model the diameter of 500, 250 and 100 microns for the outlet tubing was examined with the 1/16" (1500 μm) tubing for inlets. The length of the outlet tubing used was 10 cm. This length was observed to be the most suitable length for having a laminar flow throughout the system. Calculations are shown in appendix 1.

Results and Discussion

As was described in chapter 1, the dimensionless numbers in this research are the Reynolds number, the Peclet number and the Capillary number. Table 4.1 shows the acceptable values for these numbers in order to have mixing in the Micro-TEE reactor. The dimensionless numbers obtained with the specific boundary conditions designed for the flow in the Micro-TEE falls in the acceptable region; hence the given data can be used for the laboratory scale microfluidics system.

Table 1: Dimensionless numbers

Dimensionless numbers	Acceptable range	Aqueous phase L=0.5 cm	Monomer phase L=0.5 cm
Reynolds number	Laminar flow 1<Re<2300	187	14
Peclet number	Lower value 1<Pe<1000	89604	58
Capillary number	Low capillary number 10^{-5}	$5.43*10^{-4}$	$4.82*10^{-5}$

Table 4.1 shows the values of the dimensionless numbers obtained for the microfluidic system. Increasing of the droplet size with temperature is substantially higher for smaller channel depths than that of the larger channel depth where the heating effect becomes more significant. This results in a larger droplet size with increasing temperature (Murshed et al. 2009).

From an engineering point of view, a reaction in flow is related to the two dimensionless parameters; the Reynolds number (*Re*) and the capillary number (*Ca*). If there is no interfacial tension between water and oil, the two streams will flow along. Surface tension acts to reduce the interfacial area, and viscous stresses act to extend and drag the interface downstream. These stresses destabilize the interface and cause droplets of radius R to form. An estimate for the size of the droplets can be obtained by balancing the two stresses on the interface. The dynamics of flow-focusing bubble-forming systems is largely independent of *Ca* (capillary number) for flows with low-Reynolds number and high-Reynolds number.

Channels with length scales on the order of nanoliters to millilitres prevent the turbulent and chaotic mixing that is expected in round bottom flasks. The transition from turbulent flow to smooth flow occurs when viscous effects begin to dominate over inertial effects in the fluid.

Representing this ratio of inertial forces to viscous forces, the Reynolds number is defined as follows:

$$\mathrm{Re} = \frac{\rho v l}{\eta} \qquad 4.3$$

where ρ is the density, v is the mean velocity, l is a characteristic length scale (e.g. the diameter of the tube), and η is the dynamic viscosity.

Depending on the experimental parameters of the system, a liquid jet can transform from a thin finger of fluid to droplets. The surface area is minimized due to the Rayleigh-Plateau instability which arises when the jet becomes longer than its circumference due to perturbations and breaks up into droplets, which are typically monodisperse. The minimization of the interface is where the Capillary number effect takes over from the Re number.

A surface tension exists at the interface between the two immiscible fluids. In a two phase flowing system, the balance between this surface tension and viscous forces within the fluids dominates the structure of the fluids. Thus *Ca* is defined as follows:

$$Ca = \frac{v\eta}{\gamma} \qquad 4.4$$

where v is the mean velocity, η is the dynamic viscosity, and γ is the interfacial surface tension.

Using minor variations in the fluid properties and flow rates, one can create a series of monodisperse emulsions with different sizes. These emulsions provide an opportunity to create monodisperse beads or capsules more easily than trying to optimize a batch emulsion polymerization to be monodisperse (Zheng, Tice & Ismagilov 2004).

Generally at low values of the capillary number, monomers produce large droplets. The width of the droplet size distribution depends on the type of monomer used and the relative flowrates of the aqueous phase and oil phases. Among the various approaches to droplet-based microfluidics,

T-junction droplet-based microfluidics was used to synthesize polymeric particles in this research. Controlled emulsions formed using a T-junction microchannel made in polydimethylsiloxane (PDMS) shows that the droplet size is not dependent only on the channel width but can also be controlled by changing the input pressure gradient or flowrates of the continuous phase(Dendukuri, Doyle 2009). The important dimensionless parameters in the geometry of the Micro-TEE are the ratio of the flowrates of the continuous phase and dispersed phase, (Q_d / Q_c), these values were shown in the chapter 3.

Figure 4.4 shows the flow pattern of mixing of the monomer phase and the water phase taking place in the Micro-TEE reactor obtained by the CFD model.

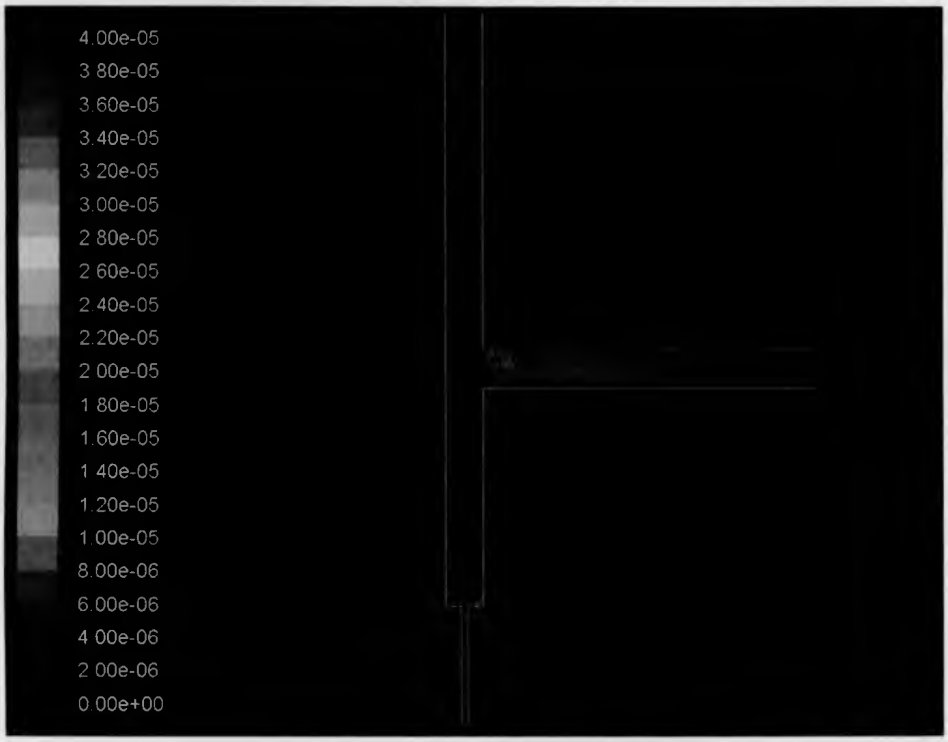

(a) Velocity vectors show the entrance of the oil phase to the T-junction where it meets the aqueous phase.

(b) Flow of the fluids in the T-junction

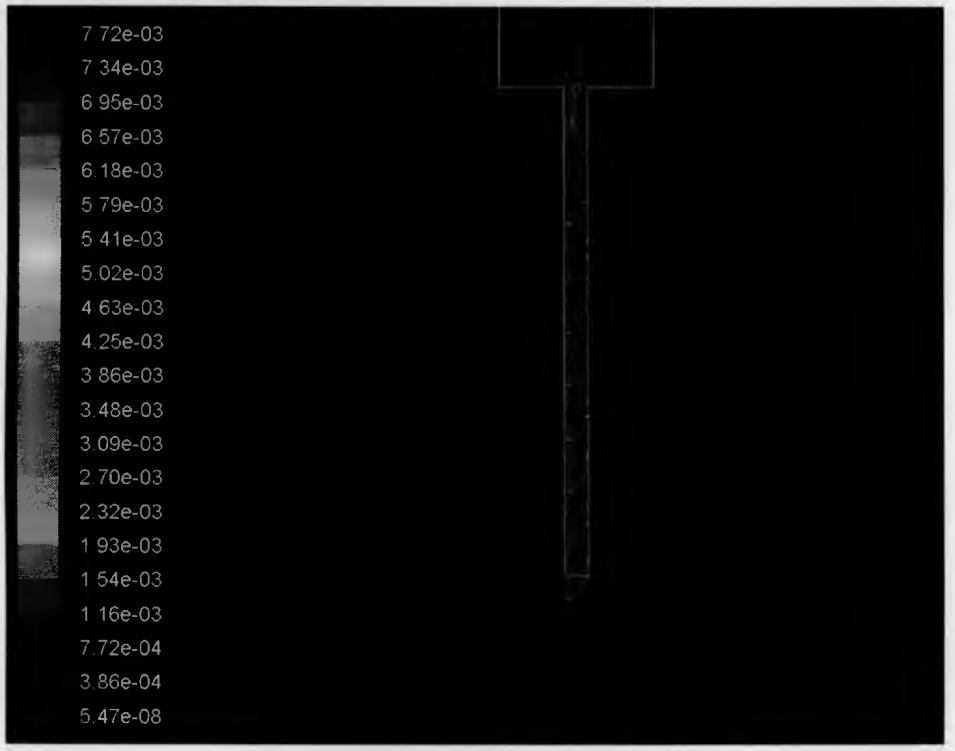

(c) Flow exiting the outlet

Figure 4: Flow pattern in the microfluidics system shown in CFD; (a) velocity vectors show the entrance of the oil phase to the T-junction where it meets the aqueous phase (b) flow of the fluids in the T-junction (c) flow exiting from the outlet.

The velocity vectors show the speed and the direction of the flow in the system, in this case in the Micro-TEE.

Therefore the above CFD model shows that the oil phase and water phase mix in the T-junction, which acts as a very good mixing reactor. The droplets formed at the outlet are the result of mixing of the oil phase and aqueous phase. Improved microspheres are obtained when reducing the diameter of the outlet tube to 100 microns. This conclusion is in agreement with the literature and the results obtained for the polymerization in the microfluidics system.

It has been confirmed in several literature studies that CFD gives excellent simulation results and is much quicker to model multiple geometries, although in this work only one geometry was discussed.